Chapter 8

A Potpourri of Particles

Although theoretical analysis of absorption and scattering by a homogeneous isotropic sphere is complicated, it is nonetheless manageable: one follows a straightforward route guided by well-known techniques in mathematical physics. Such techniques can be extended to particles of regular shape without great difficulty. The route can become more tortuous, however, if we inquire into scattering by inhomogeneous particles, or ones with anisotropic optical properties, or irregular particles. This is particularly true if the particles are neither very large nor very small compared with the wavelength.

In this chapter we consider theories of scattering by particles that are either inhomogeneous, anisotropic, or nonspherical. No attempt will be made to be comprehensive: our choice of examples is guided solely by personal taste. First we consider a special example of inhomogeneity, a layered sphere. Then we briefly discuss anisotropic spheres, including an exactly soluble problem. Isotropic optically active particles, ones with mirror asymmetry, are then considered. Cylindrical particles are not uncommon in nature—spider webs, viruses, various fibers—and we therefore devote considerable space to scattering by a right circular cylinder.

A discussion of some theoretical approaches to scattering by randomly inhomogeneous particles is followed in the final section by an outline of recent progress in constructing solutions to problems of scattering by nonspherical particles, including those of arbitrary shape.

8.1 COATED SPHERE

The field scattered by any spherically symmetrical particle composed of materials described by the constitutive relations (2.7)–(2.9) has the same form as that scattered by the homogeneous sphere considered in Chapter 4. However, the functional form of the coefficients a_n and b_n depends on the radial variation of ε and μ. In this section we consider the problem of scattering by a homogeneous sphere coated with a homogeneous layer of uniform thickness, the solution to which was first obtained by Aden and Kerker (1951). This is one of the simplest examples of a particle with a spatially variable refractive index, and it can readily be generalized to a multilayered sphere.

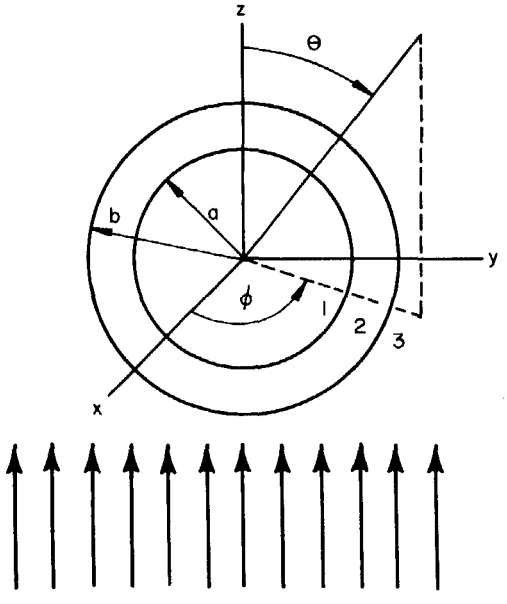

Figure 8.1 Coated sphere.

Suppose that the electromagnetic wave (4.37), (4.38) is incident on a coated sphere with inner radius a and outer radius b(Fig. 8.1). The electromagnetic field $(\mathbf{E}_1, \mathbf{H}_1)$ in the region $0 \leq r \leq a$ is given by (4.40) and the scattered field $(\mathbf{E}_s, \mathbf{H}_s)$ by (4.45). Because of the requirement of finiteness at the origin, the radial part of the functions (4.15) and (4.16), which generate the vector harmonics in the expansion of $(\mathbf{E}_1, \mathbf{H}_1)$ is constrained to be j_n. However, in the region $a \leq r \leq b$ $(a \neq 0)$, both spherical Bessel functions j_n and y_n are finite; as a consequence, the expansion of the field $(\mathbf{E}_2, \mathbf{H}_2)$ in this region is

$$\mathbf{E}_2 = \sum_{n=1}^{\infty} E_n \left[f_n \mathbf{M}_{o1n}^{(1)} - i g_n \mathbf{N}_{e1n}^{(1)} + v_n \mathbf{M}_{o1n}^{(2)} - i w_n \mathbf{N}_{e1n}^{(2)} \right],$$

$$\mathbf{H}_2 = -\frac{\mathrm{k}_2}{\omega \mu_2} \sum_{n=1}^{\infty} E_n \left[g_n \mathbf{M}_{e1n}^{(1)} + i f_n \mathbf{N}_{o1n}^{(1)} + w_n \mathbf{M}_{e1n}^{(2)} + i v_n \mathbf{N}_{o1n}^{(2)} \right],$$

where the vector harmonics $\mathbf{M}_{e1n}^{(2)}$, and so on, are generated by functions of the form (4.15) and (4.16) with radial dependence $y_n(\mathrm{k}_2 r)$. The boundary conditions

$$(\mathbf{E}_2 - \mathbf{E}_1) \times \hat{\mathbf{e}}_r = 0, \qquad (\mathbf{H}_2 - \mathbf{H}_1) \times \hat{\mathbf{e}}_r = 0, \qquad r = a$$

$$(\mathbf{E}_s + \mathbf{E}_i - \mathbf{E}_2) \times \hat{\mathbf{e}}_r = 0, \qquad (\mathbf{H}_s + \mathbf{H}_i - \mathbf{H}_2) \times \hat{\mathbf{e}}_r = 0, \qquad r = b$$

yield eight equations in the coefficients a_n, b_n, c_n, d_n, f_n, g_n, v_n, w_n:

$$\begin{aligned}
f_n m_1 \psi_n(m_2 x) - v_n m_1 \chi_n(m_2 x) - c_n m_2 \psi_n(m_1 x) &= 0,\\
w_n m_1 \chi_n'(m_2 x) - g_n m_1 \psi_n'(m_2 x) + d_n m_2 \psi_n'(m_1 x) &= 0,\\
v_n \mu_1 \chi_n'(m_2 x) - f_n \mu_1 \psi_n'(m_2 x) + c_n \mu_2 \psi_n'(m_1 x) &= 0,\\
g_n \mu_1 \psi_n(m_2 x) - w_n \mu_1 \chi_n(m_2 x) - d_n \mu_2 \psi_n(m_1 x) &= 0,\\
m_2 \psi_n'(y) - a_n m_2 \xi_n'(y) - g_n \psi_n'(m_2 y) + w_n \chi_n'(m_2 y) &= 0, \qquad (8.1)\\
m_2 b_n \xi_n(y) - m_2 \psi_n(y) + f_n \psi_n(m_2 y) - v_n \chi_n(m_2 y) &= 0,\\
\mu_2 \psi_n(y) - a_n \mu_2 \xi_n(y) - g_n \mu \psi_n(m_2 y) + w_n \mu \chi_n(m_2 y) &= 0,\\
b_n \mu_2 \xi_n'(y) - \mu_2 \psi_n'(y) + f_n \mu \psi_n'(m_2 y) - v_n \mu \chi_n'(m_2 y) &= 0,
\end{aligned}$$

where m_1 and m_2 are the refractive indices of the core and coating relative to the surrounding medium; μ, μ_1, μ_2 are the permeabilities of the surrounding medium, core, and coating; and $x = ka$, $y = kb$. The Riccati–Bessel function $\chi_n(z)$ is $-zy_n(z)$. Let us assume for simplicity that $\mu = \mu_1 = \mu_2$ and solve the set of equations (8.1) for the scattering coefficients a_n and b_n:

$$a_n = \frac{\psi_n(y)[\psi_n'(m_2 y) - A_n \chi_n'(m_2 y)] - m_2 \psi_n'(y)[\psi_n(m_2 y) - A_n \chi_n(m_2 y)]}{\xi_n(y)[\psi_n'(m_2 y) - A_n \chi_n'(m_2 y)] - m_2 \xi_n'(y)[\psi_n(m_2 y) - A_n \chi_n(m_2 y)]},$$

$$b_n = \frac{m_2 \psi_n(y)[\psi_n'(m_2 y) - B_n \chi_n'(m_2 y)] - \psi_n'(y)[\psi_n(m_2 y) - B_n \chi_n(m_2 y)]}{m_2 \xi_n(y)[\psi_n'(m_2 y) - B_n \chi_n'(m_2 y)] - \xi_n'(y)[\psi_n(m_2 y) - B_n \chi_n(m_2 y)]},$$

$$A_n = \frac{m_2 \psi_n(m_2 x) \psi_n'(m_1 x) - m_1 \psi_n'(m_2 x) \psi_n(m_1 x)}{m_2 \chi_n(m_2 x) \psi_n'(m_1 x) - m_1 \chi_n'(m_2 x) \psi_n(m_1 x)},$$

$$B_n = \frac{m_2 \psi_n(m_1 x) \psi_n'(m_2 x) - m_1 \psi_n(m_2 x) \psi_n'(m_1 x)}{m_2 \chi_n'(m_2 x) \psi_n(m_1 x) - m_1 \psi_n'(m_1 x) \chi_n(m_2 x)}. \qquad (8.2)$$

A program for computing a_n and b_n is given in Appendix B.

If $m_1 = m_2$, then $A_n = B_n = 0$ and the coefficients (8.2) reduce to those for a homogeneous sphere. We also have $\lim_{a \to 0} A_n = \lim_{a \to 0} B_n = 0$; therefore, in the limit of zero core radius the coefficients (8.2) reduce to those for a homogeneous sphere of radius b and relative refractive index m_2, as required. When $m_2 = 1$, the coefficients reduce to those for a sphere of radius a and relative refractive index m_1; this gives us yet another check on the correctness of our solution.

8.2 ANISOTROPIC SPHERE

We have discussed *intrinsically* anisotropic particles—ones with anisotropy originating in their optical constants rather than their shape—in previous chapters. In Section 5.6 we gave the solution to the problem of scattering by an anisotropic sphere in the Rayleigh approximation. From the results of that section and Section 5.5 it follows that the average cross section $\langle C \rangle$ (scattering or absorption) of a collection of randomly oriented, *sufficiently small*, anisotropic spheres is

$$\langle C \rangle = \tfrac{1}{3}C_1 + \tfrac{1}{3}C_2 + \tfrac{1}{3}C_3, \tag{8.3}$$

where C_j is the cross section for an isotropic sphere with dielectric function ϵ_j, one of the three distinct (in general) principal values of the dielectric function tensor. Equation (8.3) has been used not only for spheres small compared with the wavelength but for larger spheres as well. Perhaps (8.3) is valid without qualification (although we believe otherwise); nevertheless, to our knowledge this has never been demonstrated. The reason for this is that no exact solution to the problem of scattering by an anisotropic sphere of arbitrary radius has been published. Therefore, it is difficult to determine by computations the limits of validity—if any—of (8.3). In the absence of an exact theory, we are forced to fall back on physical reasoning to make an educated guess about the conditions under which (8.3) might be expected to fail.

Let us consider for simplicity a sphere composed of a uniaxial material (see Section 9.3). We denote by $k_{\parallel}$ and $k_{\perp}$ the wave numbers corresponding to the two principal values of the dielectric function tensor. It is reasonable to assert on physical grounds that anisotropy is only a perturbation if

$$|(k_{\parallel} - k_{\perp})a| \ll 1,$$

where a is the radius of the sphere; that is, the two kinds of plane waves that can propagate in a uniaxial material undergo the same change in phase and amplitude over a distance comparable with the size of the particle. A corollary of this is that the effect of anisotropy becomes appreciable when

$$|(k_{\parallel} - k_{\perp})a| > 1,$$

and if this condition holds, one cannot reasonably expect to obtain the solution to the anisotropic sphere problem by patching together solutions for an isotropic sphere. We emphasize, however, that this criterion is only our best guess in the absence of anything better.

The reason for the intractability of the anisotropic sphere scattering problem is the fundamental mismatch between the symmetry of the optical constants and the shape of the particle. For example, the vector wave equation for a uniaxial material is separable in cylindrical coordinates; that is, the solutions to the field equations are cylindrical waves. But the bounding surface of the

particle is a sphere, and troubles arise when we try to satisfy the boundary conditions. Thus, techniques for extending the theory of scattering by an anisotropic sphere beyond the Rayleigh limit are not likely to be based on separation of variables.

A special anisotropic particle scattering problem has been treated by Roth and Dignam (1973), who considered an isotropic sphere coated with a uniform film with constitutive relations

$$D_r = \varepsilon_n E_r, \qquad D_\theta = \varepsilon_t E_\theta, \qquad D_\phi = \varepsilon_t E_\phi, \tag{8.4}$$

where the permittivities ε_n and ε_t are independent of position and (E_r, E_θ, E_ϕ) are the field components relative to a spherical polar coordinate system. The constitutive relations (8.4) may be interpreted as applying to an oriented layer, or one that is "locally uniaxial." The solution to this problem is exact, but involves Bessel functions of complex *order*. Computation of ordinary Bessel functions is difficult enough, but mere contemplation of complex-order Bessel functions is sufficient to make strong men weep. It is perhaps for these apparent computational difficulties that the ramifications of the solution of Roth and Dignam have not been fully explored.

8.3 OPTICALLY ACTIVE PARTICLES

Almost all the particles we have considered have been composed of linear isotropic media described by the constitutive relations (2.7)–(2.9), which are not universally valid. Unfortunately, as soon as we depart from these relations we are usually confronted with problems that are not exactly soluble. However, exact solutions are obtainable for particles of regular geometrical shape composed of isotropic, *optically active* media. Such media are ones in which plane harmonic waves can propagate without change in polarization, but only if they are circularly polarized with either handedness; the complex refractive indices for left-circularly and right-circularly polarized waves are different. A simple conceptual model of an isotropic, optically active medium is a random array of screws, which is invariant under rotation through any angle, but under reflection the handedness of the screws changes. An example of an isotropic, optically active particle is a sugar-water drop.

The constitutive relations

$$\mathbf{D} = \varepsilon\mathbf{E} + \gamma\varepsilon\nabla \times \mathbf{E}, \qquad \mathbf{B} = \mu\mathbf{H} + \beta\mu\nabla \times \mathbf{H}, \tag{8.5}$$

where ε, μ, γ, and β are scalar phenomenological coefficients, are sufficient for a macroscopic description of optical activity. That is, plane homogeneous electromagnetic waves can propagate in media described by (8.5) only if they are circularly polarized. If we take γ and β to be equal, the phenomenological coefficients are related to the complex refractive indices N_L and N_R by

$$\beta = \frac{1}{2}\left(\frac{1}{\mathrm{k}_R} - \frac{1}{\mathrm{k}_L}\right), \qquad \omega\sqrt{\varepsilon\mu} = \frac{1}{\frac{1}{2}(1/\mathrm{k}_R + 1/\mathrm{k}_L)},$$

where the wave numbers k_L and k_R are

$$k_L = \frac{2\pi}{\lambda} N_L, \qquad k_R = \frac{2\pi}{\lambda} N_R.$$

If we assume harmonic time dependence $e^{-i\omega t}$, the Maxwell equations (2.1)–(2.4) may be written

$$\nabla \cdot \left(\mathbf{D} + \frac{i}{\omega}\mathbf{J}_F\right) = 0, \qquad \nabla \cdot \mathbf{B} = 0, \tag{8.6}$$

$$\nabla \times \mathbf{E} - i\omega\mathbf{B} = 0, \qquad \nabla \times \mathbf{H} + i\omega\left(\mathbf{D} + \frac{i}{\omega}\mathbf{J}_F\right) = 0. \tag{8.7}$$

Note that $\mathbf{D}$ and $\mathbf{J}_F$ do not appear separately in (8.6) and (8.7) but only in the combination $\mathbf{D} + i\mathbf{J}_F/\omega$, which we may interpret as the total electric displacement and assume that $\mathbf{D}$ in (8.5) is this quantity. In fact, we could have done this in previous chapters but refrained from doing so because the notion of conductivity is well established. However, it is not possible to determine from macroscopic experiments of the type discussed in this book if the imaginary part of the refractive index originates from "free" or "bound" charge currents. Thus, we need not make separate assumptions about the relations between $\mathbf{D}$ and $\mathbf{E}$ and between $\mathbf{J}_F$ and $\mathbf{E}$.

The constitutive relations (8.5) and the field equations (8.6), (8.7) can be written compactly in matrix form:

$$\nabla^2\begin{pmatrix}\mathbf{E}\\ \mathbf{H}\end{pmatrix} + \mathsf{K}^2\begin{pmatrix}\mathbf{E}\\ \mathbf{H}\end{pmatrix} = 0,$$

$$\nabla \times \begin{pmatrix}\mathbf{E}\\ \mathbf{H}\end{pmatrix} = \mathsf{K}\begin{pmatrix}\mathbf{E}\\ \mathbf{H}\end{pmatrix},$$

$$\nabla \cdot \begin{pmatrix}\mathbf{E}\\ \mathbf{H}\end{pmatrix} = 0,$$

$$\mathsf{K} = \frac{i\omega}{1 - \beta^2\varepsilon\mu\omega^2}\begin{pmatrix}-i\beta\varepsilon\mu\omega & \mu\\ -\varepsilon & -i\beta\varepsilon\mu\omega\end{pmatrix}. \tag{8.8}$$

We often refer to the electromagnetic field and then go on to treat the electric and magnetic fields as separate entities, a slight inconsistency. However, we have shown that the field equations can be written in such a way that the electromagnetic field, the column vector with elements $\mathbf{E}$ and $\mathbf{H}$, is treated as a single entity. Thus, (8.8) has an aesthetic appeal, which transcends its immediate usefulness to the problem at hand.

A linear transformation of the electromagnetic field

$$\begin{pmatrix}\mathbf{E}\\ \mathbf{H}\end{pmatrix} = \mathsf{A}\begin{pmatrix}\mathbf{Q}_L\\ \mathbf{Q}_R\end{pmatrix} \tag{8.9}$$

diagonalizes K:

$$\Lambda = \mathsf{A}^{-1}\mathsf{K}\mathsf{A},$$

where

$$\Lambda = \begin{pmatrix} k_L & 0 \\ 0 & -k_R \end{pmatrix}, \qquad A = \begin{pmatrix} 1 & a_R \\ a_L & 1 \end{pmatrix},$$

$$a_R = -i\sqrt{\mu/\epsilon}, \qquad a_L = -i\sqrt{\epsilon/\mu}.$$

The transformed fields $\mathbf{Q}_L$ and $\mathbf{Q}_R$ independently satisfy equations of the form

$$\nabla^2\mathbf{Q} + k^2\mathbf{Q} = 0, \tag{8.10}$$

$$\nabla \times \mathbf{Q} = k\mathbf{Q}, \tag{8.11}$$

$$\nabla \cdot \mathbf{Q} = 0, \tag{8.12}$$

where $k = k_L$ for $\mathbf{Q} = \mathbf{Q}_L$ and $k = -k_R$ for $\mathbf{Q} = \mathbf{Q}_R$. Therefore, the most general electromagnetic wave in an optically active medium is a superposition of waves of left-handed and right-handed types.

At the beginning of this section we stated, without proof, that only circularly polarized plane waves can propagate in media described by the constitutive relations (8.5). It is now a relatively easy matter to show that this is so. Let us consider plane homogeneous waves $\exp(i\mathbf{k} \cdot \mathbf{x})$ propagating in the $\hat{\mathbf{e}}$ direction, where $\mathbf{k} = k\hat{\mathbf{e}}$. From (8.11) we have $i\hat{\mathbf{e}} \times \mathbf{Q} = \pm\mathbf{Q}$, and the transversality condition (8.12) implies that $\hat{\mathbf{e}} \cdot \mathbf{Q} = 0$. Therefore, we can write $\mathbf{Q} = Q_{\parallel}\hat{\mathbf{e}}_{\parallel} + Q_{\perp}\hat{\mathbf{e}}_{\perp}$, where $\hat{\mathbf{e}} \times \hat{\mathbf{e}}_{\perp} = \hat{\mathbf{e}}_{\parallel}$ and $\hat{\mathbf{e}} \times \hat{\mathbf{e}}_{\parallel} = -\hat{\mathbf{e}}_{\perp}$, which yields

$$\mathbf{Q} = Q_{\parallel}(\hat{\mathbf{e}}_{\parallel} \pm i\hat{\mathbf{e}}_{\perp}),$$

where the plus sign holds when $\mathbf{Q} = \mathbf{Q}_R$ and the minus when $\mathbf{Q} = \mathbf{Q}_L$. We showed in Section 2.11 that $\hat{\mathbf{e}}_{\parallel} + i\hat{\mathbf{e}}_{\perp}$ represents a right-circularly polarized wave and $\hat{\mathbf{e}}_{\parallel} - i\hat{\mathbf{e}}_{\perp}$ a left-circularly polarized wave. Thus, it is clear that plane wave solutions to the field equations (8.10)–(8.12) are necessarily circularly polarized. In general, therefore, it is natural to refer to $\mathbf{Q}_L$ as a wave of left-handed type and $\mathbf{Q}_R$ as a wave of right-handed type.

Consider now the field scattered by an isotropic, optically active sphere of radius a, which is embedded in a nonactive medium with wave number k and illuminated by an x-polarized wave. Most of the groundwork for the solution to this problem has been laid in Chapter 4, where the expansions (4.37) and (4.38) of the incident electric and magnetic fields are given. Equation (8.11) requires that the expansion functions for $\mathbf{Q}$ be of the form $\mathbf{M} \pm \mathbf{N}$; therefore, the vector spherical harmonics expansions of the fields inside the sphere are

$$\mathbf{Q}_L = \sum_{n=1}^{\infty} E_n\{f_{on}[\mathbf{M}_{o1n}^{(1)}(k_L) + \mathbf{N}_{o1n}^{(1)}(k_L)] + f_{en}[\mathbf{M}_{e1n}^{(1)}(k_L) + \mathbf{N}_{e1n}^{(1)}(k_L)]\},$$

$$\mathbf{Q}_R = \sum_{n=1}^{\infty} E_n\{g_{on}[\mathbf{M}_{o1n}^{(1)}(k_R) - \mathbf{N}_{o1n}^{(1)}(k_R)] + g_{en}[\mathbf{M}_{e1n}^{(1)}(k_R) - \mathbf{N}_{e1n}^{(1)}(k_R)]\}, \tag{8.13}$$

where $E_n = E_0 i^n(2n+1)/n(n+1)$ and k_R or k_L in the argument of the vector harmonics indicates that $\rho = k_R r$ or $\rho = k_L r$ are the arguments of the spherical Bessel function $j_n(\rho)$ in the generating functions for these harmonics. The expansions of the scattered field are

$$\mathbf{E}_s = \sum_{n=1}^{\infty} E_n\left[ia_n\mathbf{N}_{eln}^{(3)} - b_n\mathbf{M}_{oln}^{(3)} + c_n\mathbf{M}_{eln}^{(3)} - id_n\mathbf{N}_{oln}^{(3)}\right],$$

$$\mathbf{H}_s = \frac{k}{\omega\mu}\sum_{n=1}^{\infty} E_n\left[a_n\mathbf{M}_{eln}^{(3)} + ib_n\mathbf{N}_{oln}^{(3)} - ic_n\mathbf{N}_{eln}^{(3)} - d_n\mathbf{M}_{oln}^{(3)}\right].$$

The electromagnetic field $(\mathbf{E}_1, \mathbf{H}_1)$ inside the sphere is obtained from (8.13) and the transformation (8.9). We saw in Chapter 4 that, for given n, there are four unknown coefficients in the expansions for the fields when the sphere is nonactive; optical activity doubles the number of coefficients, which are determined by applying the conditions (4.39) at the boundary between sphere and surrounding medium and solving the resulting system of eight linear equations. We are interested primarily in the coefficients of the scattered field:

$$a_n = \frac{V_n(R)A_n(L) + V_n(L)A_n(R)}{W_n(L)V_n(R) + V_n(L)W_n(R)},$$

$$b_n = \frac{W_n(L)B_n(R) + W_n(R)B_n(L)}{W_n(L)V_n(R) + V_n(L)W_n(R)},$$

$$c_n = i\frac{W_n(R)A_n(L) - W_n(L)A_n(R)}{W_n(L)V_n(R) + V_n(L)W_n(R)} = -d_n,$$

$$W_n(J) = m\psi_n(m_J x)\xi_n'(x) - \xi_n(x)\psi_n'(m_J x),$$

$$V_n(J) = \psi_n(m_J x)\xi_n'(x) - m\xi_n(x)\psi_n'(m_J x),$$

$$A_n(J) = m\psi_n(m_J x)\psi_n'(x) - \psi_n(x)\psi_n'(m_J x),$$

$$B_n(J) = \psi_n(m_J x)\psi_n'(x) - m\psi_n(x)\psi_n'(m_J x).$$

J is L or R. The relative refractive indices m_L, m_R and the mean refractive index m are defined as follows:

$$m_L = \frac{N_L}{N}, \qquad m_R = \frac{N_R}{N}, \qquad \frac{1}{m} = \frac{1}{2}\left(\frac{1}{m_R} + \frac{1}{m_L}\right)\frac{\mu_1}{\mu},$$

where N is the refractive index and μ the permeability of the surrounding medium. The difference Δm between the refractive indices m_R and m_L is usually small; therefore, m is $(m_R + m_L)/2$ to terms of order $(\Delta m)^2$ (we have also assumed that $\mu_1 = \mu$). If there is no optical activity ($m_L = m_R$), then a_n and b_n reduce to (4.53) and c_n vanishes identically.

8.3.1 Matrix Elements and Cross Sections

In Section 4.4 we showed that the off-diagonal elements of the amplitude scattering matrix (3.12) are zero for a nonactive sphere. If the sphere is optically active, however, the matrix elements are

$$S_1 = \sum_n \frac{2n+1}{n(n+1)}(a_n\pi_n + b_n\tau_n),$$

$$S_2 = \sum_n \frac{2n+1}{n(n+1)}(a_n\tau_n + b_n\pi_n),$$

$$S_3 = \sum_n \frac{2n+1}{n(n+1)}c_n(\pi_n + \tau_n) = -S_4.$$

In problems involving optically active particles it is usually more convenient to use the amplitude scattering matrix in the circular polarization representation. The transformation from linearly to circularly polarized electric field components is

$$\begin{pmatrix} E_L \\ E_R \end{pmatrix} = \frac{1}{\sqrt{2}}\begin{pmatrix} 1 & i \\ 1 & -i \end{pmatrix}\begin{pmatrix} E_\parallel \\ E_\perp \end{pmatrix}, \tag{8.14}$$

and the inverse transformation is

$$\begin{pmatrix} E_\parallel \\ E_\perp \end{pmatrix} = \frac{1}{\sqrt{2}}\begin{pmatrix} 1 & 1 \\ -i & i \end{pmatrix}\begin{pmatrix} E_L \\ E_R \end{pmatrix}. \tag{8.15}$$

If the fields in (3.12) are transformed according to (8.14) and (8.15), the relation between incident and scattered fields becomes

$$\begin{pmatrix} E_{Ls} \\ E_{Rs} \end{pmatrix} = \frac{e^{ik(r-z)}}{-ikr}\begin{pmatrix} S_{2c} & S_{3c} \\ S_{4c} & S_{1c} \end{pmatrix}\begin{pmatrix} E_{Li} \\ E_{Ri} \end{pmatrix},$$

$$S_{1c} = \tfrac{1}{2}(S_2 + S_1 - iS_4 + iS_3),$$

$$S_{2c} = \tfrac{1}{2}(S_2 + S_1 + iS_4 - iS_3),$$

$$S_{3c} = \tfrac{1}{2}(S_2 - S_1 + iS_4 + iS_3),$$

$$S_{4c} = \tfrac{1}{2}(S_2 - S_1 - iS_4 - iS_3).$$

This relation is not restricted to a specific particle; for an optically active sphere, however, two of the matrix elements are equal: $S_{3c} = S_{4c}$.

The (4×4) scattering matrix elements (3.16) for an optically active sphere satisfy the following six relations:

$$S_{31} = -S_{13}, \qquad S_{32} = -S_{23}, \qquad S_{43} = -S_{34},$$
$$S_{41} = S_{14}, \qquad S_{42} = S_{24}, \qquad S_{21} = S_{12}. \tag{8.16}$$

The cross sections for extinction and scattering by an optically active particle are different for incident left-circularly and right-circularly polarized light. For an optically active sphere, the cross sections can be obtained in a manner similar to that for a nonactive sphere (Section 4.4). Therefore, we give only the results and omit the details:

$$C_{\text{sca},L} = \frac{2\pi}{k^2} \sum_{n=1}^{\infty} (2n+1)\left[|a_n|^2 + |b_n|^2 + 2|c_n|^2 - 2\,\text{Im}\{(a_n + b_n)c_n^*\}\right],$$

$$C_{\text{sca},R} = \frac{2\pi}{k^2} \sum_{n=1}^{\infty} (2n+1)\left[|a_n|^2 + |b_n|^2 + 2|c_n|^2 + 2\,\text{Im}\{(a_n + b_n)c_n^*\}\right],$$

$$C_{\text{ext},L} = \frac{4\pi}{k^2}\,\text{Re}\{S_L\} = \frac{2\pi}{k^2} \sum_{n=1}^{\infty} (2n+1)\text{Re}\{a_n + b_n - 2ic_n\},$$

$$C_{\text{ext},R} = \frac{4\pi}{k^2}\,\text{Re}\{S_R\} = \frac{2\pi}{k^2} \sum_{n=1}^{\infty} (2n+1)\text{Re}\{a_n + b_n + 2ic_n\}, \tag{8.17}$$

where $S_L = S_{2c}(0°)$ and $S_R = S_{1c}(0°)$ are the amplitude scattering matrix elements in the forward direction.

8.3.2 Circular Dichroism and Optical Rotation

We have shown that only circularly polarized waves may propagate in optically active media without change in their state of polarization. However, the

polarization of a wave that is *linearly* polarized at a particular point, say $z = 0$, changes continuously as it propagates in the z direction. At $z = h$ the wave will be *elliptically* polarized with ellipticity $|\Theta_T|$, and the azimuth of the vibration ellipse will have rotated through an angle Φ_T relative to the direction of polarization at $z = 0$. These quantities are related to the complex refractive indices $N_L = n_L + ik_L$ and $N_R = n_R + ik_R$ for left-circularly and right-circularly polarized waves by

$$\Phi_T + i\Theta_T = \frac{\pi}{\lambda}(N_L - N_R)h,$$

provided that $|2\pi(k_L - k_R)h/\lambda| \ll 1$. If Φ_T is positive the vibration ellipse rotates in the clockwise sense.

A medium is said to be *circularly dichroic*—it absorbs differently according to the state of circular polarization of the light—if $k_L - k_R \neq 0$; it is *circularly birefringent*, which is manifested by *optical rotation*, if $n_L - n_R \neq 0$. Optical rotation and circular dichroism are not independent phenomena, but are connected by Kramers–Kronig relations:

$$\begin{aligned} \phi(\omega) &= \frac{2\omega^2}{\pi} P\int_0^\infty \frac{\theta(\Omega)}{\Omega(\Omega^2 - \omega^2)}\, d\Omega, \\ \theta(\omega) &= \frac{-2\omega}{\pi} P\int_0^\infty \frac{\phi(\Omega)}{\Omega^2 - \omega^2}\, d\Omega, \end{aligned} \tag{8.18}$$

where $\phi = \Phi_T/h$ and $\theta = \Theta_T/h$ are the rotation and change of ellipticity per unit path length. A derivation of (8.18) in the same spirit as the derivations of dispersion relations in Section 2.3 has been given by Emeis et al. (1967). Note that (8.18) do not follow by naively applying the dispersion relations (2.49) and (2.50) to N_L and N_R separately and then subtracting the resulting expressions; the reasons for this have been discussed by Smith (1976).

Circular dichroism and optical rotation for *particulate* media may be operationally defined in terms of the Stokes parameters (2.80), which in the circular polarization representation are written

$$\begin{aligned} I &= E_L E_L^* + E_R E_R^*, & Q &= E_L^* E_R + E_R^* E_L, \\ U &= i(E_L^* E_R - E_L E_R^*), & V &= E_R E_R^* - E_L E_L^*. \end{aligned} \tag{8.19}$$

The azimuth γ and ellipticity $|\tan\eta|$ of the vibration ellipse for an arbitrary beam can be determined from the Stokes parameters by (2.82).

If optical rotation Φ_T for a collection of particles is defined as the change in azimuth of a horizontally polarized incident beam ($\gamma_i = 0$) after it is

transmitted through this medium, then

$$\Phi_T = \gamma_t - \gamma_i = \tfrac{1}{2}\tan^{-1}\frac{U_t}{Q_t}, \tag{8.20}$$

where subscripts i and t denote incident and transmitted beams. Similarly, if circular dichroism Θ_T for the particulate medium is defined as the change in ellipticity of a horizontally polarized beam ($\eta_i = 0$) after it is transmitted through the medium, then

$$\Theta_T = \tan\eta_t; \qquad \eta_t = \tfrac{1}{2}\tan^{-1}\frac{V_t}{\sqrt{Q_t^2 + U_t^2}}. \tag{8.21}$$

Note that these definitions of optical rotation and circular dichroism for a particulate medium depend on the choice of the horizontal direction unless the medium is invariant with respect to arbitrary rotation about an axis parallel to the incident beam.

Equations (8.20) and (8.21) are completely general; no assumptions have been made about the nature of the particles. Let us now consider a more specific example: $\mathfrak{N}$ *identical* particles per unit volume of a slab of thickness h; the medium surrounding the particles is nonabsorbing and nonactive. If the amplitude scattering matrix in the circular polarization representation is diagonal in the forward direction [$S_{3c}(0°) = S_{4c}(0°) = 0$], then by following a line of reasoning similar to that which led to (3.39) we obtain the left-handed and right-handed components of the transmitted electric field:

$$\begin{aligned} E_L &= \frac{1}{\sqrt{2}}E\left(1 - \frac{2\pi}{k^2}\mathfrak{N}S_L h\right), \\ E_R &= \frac{1}{\sqrt{2}}E\left(1 - \frac{2\pi}{k^2}\mathfrak{N}S_R h\right), \end{aligned} \tag{8.22}$$

where $E = E_0\exp(ikz)$ is the incident electric field. We have also assumed in the derivation of (8.22) that $|2\pi\,\mathfrak{N}Sh/k^2| \ll 1$. If the Stokes parameters (8.19) corresponding to (8.22) are inserted into (8.20) and (8.21), we obtain

$$\phi + i\theta = \frac{\pi}{k^2}\mathfrak{N}i(S_L - S_R). \tag{8.23}$$

Thus, the difference between the diagonal elements of the forward amplitude scattering matrix in the circular polarization representation has a simple physical interpretation. Although we considered identical particles for conveni-

ence, (8.23) is readily generalized to a suspension of nonidentical particles: the optical rotation and circular dichroism of such a suspension is merely the sum of the contributions from the individual components. We may also relax the requirement that $|2\pi\mathcal{N}Sh/k^2| \ll 1$ provided that multiple scattering is negligible; see the discussion following (3.46).

If the particles are homogeneous spheres, then from the results of the preceding section we have

$$i(S_L - S_R) = 2S_3(0°) = 2\sum_{n=1}^{\infty}(2n+1)c_n. \tag{8.24}$$

It also follows from (8.17) and (8.23) that the circular dichroism of a suspension of spheres is proportional to the difference between the extinction cross sections for left-circularly and right-circularly polarized light:

$$\theta = \tfrac{1}{4}\mathcal{N}(C_{\text{ext},L} - C_{\text{ext},R}) = \theta_{\text{sca}} + \theta_{\text{abs}},$$

$$\theta_{\text{sca}} = \tfrac{1}{4}\mathcal{N}(C_{\text{sca},L} - C_{\text{sca},R}), \qquad \theta_{\text{abs}} = \tfrac{1}{4}\mathcal{N}(C_{\text{abs},L} - C_{\text{abs},R}). \tag{8.25}$$

However, (8.25) is not restricted to spheres but holds for particles of arbitrary shape. Thus, circular dichroism in particulate media includes a component that is the result of differential scattering, in contrast with circular dichroism in homogeneous media, which arises solely from differential absorption of left-circularly and right-circularly polarized light.

If the spheres are sufficiently small ($x \ll 1$, $|mx| \ll 1$), the series (8.24) can be truncated after the first term; the leading coefficient correct to terms of order x^3 is

$$c_1 = \frac{x^3}{3}\frac{m_L - m_R}{m^2 + 2},$$

where we have used the series expansions (5.3) of the various Bessel functions and their derivatives. Therefore, (8.23) in the small particle limit is

$$\phi + i\theta = f\frac{\pi}{\lambda}(N_L - N_R)\frac{3}{m^2 + 2},$$

where $f = 4\pi a^3\mathcal{N}/3$ is the fraction of the suspension volume occupied by the particles. The quantity $\pi(N_L - N_R)/\lambda$ is the intrinsic optical rotation and circular dichroism of the spheres; $3/(m^2 + 2)$ may be interpreted as the effect of the surrounding medium—a "solvent" correction.

If m, the average relative refractive index, varies only slightly over the frequency region of interest, then the circular dichroism (CD) spectrum $\theta(\omega)$ and the optical rotatory dispersion (ORD) spectrum $\phi(\omega)$ of spheres small compared with the wavelength are essentially the same as those of the

homogeneous parent material. But this is not necessarily true for spheres, or particles of any shape, comparable with or larger than the wavelength. Indeed, CD (or ORD) spectra for the same material in the homogeneous and particulate states may bear little resemblance to each other. This has important implications for interpreting CD and ORD spectra of biological particles.

8.4 INFINITE RIGHT CIRCULAR CYLINDER

There are many naturally occurring particles, such as some viruses and asbestos fibers, which are best represented as cylinders long compared with their diameter. Therefore, in this section we shall construct the exact solution to the problem of absorption and scattering by an infinitely long right circular cylinder and examine some of the properties of this solution.

As in the problem of scattering by a sphere (Chapter 4), our starting point is the scalar wave equation $\nabla^2\psi + k^2\psi = 0$, which in cylindrical polar coordinates r, ϕ, z(Fig. 8.2) is

$$\frac{1}{r}\frac{\partial}{\partial r}\left(r\frac{\partial\psi}{\partial r}\right) + \frac{1}{r^2}\frac{\partial^2\psi}{\partial\phi^2} + \frac{\partial^2\psi}{\partial z^2} + k^2\psi = 0. \tag{8.26}$$

Separable solutions to (8.26) that are single-valued functions of ϕ are of the form

$$\psi_n(r, \phi, z) = Z_n(\rho)e^{in\phi}e^{ihz} \qquad (n = 0, \pm 1, \ldots), \tag{8.27}$$

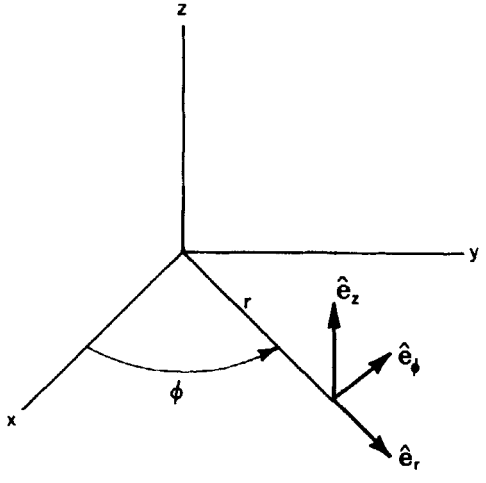

Figure 8.2 Cylindrical polar coordinate system. The z axis lies along the axis of the infinite cylinder.

where $\rho = r\sqrt{k^2 - h^2}$ and Z_n is a solution to the Bessel equation

$$\rho \frac{d}{d\rho}\left(\rho \frac{d}{d\rho} Z_n\right) + (\rho^2 - n^2) Z_n = 0. \tag{8.28}$$

The linearly independent solutions to (8.28) are the Bessel functions of first and second kind, J_n and Y_n, of integral order n. In general, the separation constant h is unrestricted, although in the problems with which we shall deal, h is dictated by the form of the incident field and the necessity of satisfying the conditions (3.7) at the boundary between the cylinder and the surrounding medium.

The vector cylindrical harmonics generated by (8.27) are

$$\mathbf{M}_n = \nabla \times (\hat{\mathbf{e}}_z \psi_n), \qquad \mathbf{N}_n = \frac{\nabla \times \mathbf{M}_n}{k},$$

where we have taken as pilot vector the unit vector $\hat{\mathbf{e}}_z$ parallel to the cylinder axis (Fig. 8.3). In component form these vector harmonics are

$$\mathbf{M}_n = \sqrt{k^2 - h^2}\left(in \frac{Z_n(\rho)}{\rho} \hat{\mathbf{e}}_r - Z_n'(\rho)\hat{\mathbf{e}}_\phi\right) e^{i(n\phi + hz)},$$

$$\mathbf{N}_n = \frac{\sqrt{k^2 - h^2}}{k}\left(ihZ_n'(\rho)\hat{\mathbf{e}}_r - hn \frac{Z_n(\rho)}{\rho} \hat{\mathbf{e}}_\phi + \sqrt{k^2 - h^2}\, Z_n(\rho)\hat{\mathbf{e}}_z\right) e^{i(n\phi + hz)}.$$

The vector harmonics are orthogonal in the sense that

$$\int_0^{2\pi} \mathbf{M}_n \cdot \mathbf{M}_m^* \, d\phi = \int_0^{2\pi} \mathbf{N}_n \cdot \mathbf{N}_m^* \, d\phi = \int_0^{2\pi} \mathbf{M}_n \cdot \mathbf{N}_m^* \, d\phi = 0 \qquad (n \neq m).$$

Let us now consider an infinite right circular cylinder of radius a, which is illuminated by a plane homogeneous wave $\mathbf{E}_i = \mathbf{E}_0 e^{ik\hat{\mathbf{e}}_i \cdot \mathbf{x}}$ propagating in the direction $\hat{\mathbf{e}}_i = -\sin\zeta\hat{\mathbf{e}}_x - \cos\zeta\hat{\mathbf{e}}_z$, where ζ is the angle between the incident wave and the cylinder axis (Fig. 8.3). There are two possible orthogonal polarization states of the incident wave: electric field polarized *parallel* to the xz plane; and electric field polarized *perpendicular* to the xz plane. We shall consider each of these polarizations in turn.

Case I. Incident Electric Field Parallel to the xz Plane. The first step is to expand the incident electric field

$$\mathbf{E}_i = E_0(\sin\zeta\hat{\mathbf{e}}_z - \cos\zeta\hat{\mathbf{e}}_x) e^{-ik(r\sin\zeta\cos\phi + z\cos\zeta)}$$

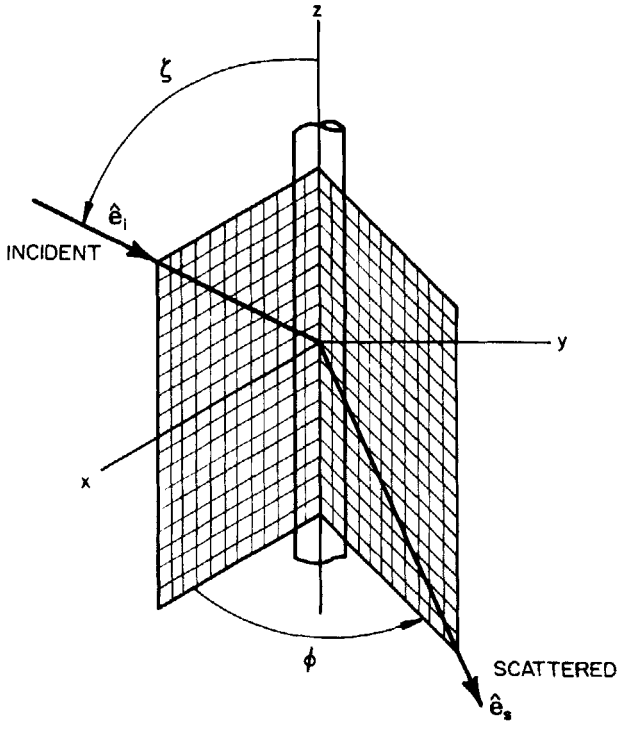

Figure 8.3 Infinite cylinder obliquely illuminated by a plane wave.

in vector cylindrical harmonics. In order for the expansion to be finite at $r = 0$ we must exclude the Bessel function Y_n as the radially dependent part of the generating function; it is also clear from the form of $\mathbf{E}_i$ that h in (8.27) must be $-\mathrm{k}\cos\zeta$. Thus, the expansion of $\mathbf{E}_i$ is

$$\mathbf{E}_i = \sum_{n=-\infty}^{\infty} \left[A_n \mathbf{M}_n^{(1)} + B_n \mathbf{N}_n^{(1)}\right],$$

where the vector harmonics are generated by $J_n(\mathrm{k}r\sin\zeta)e^{in\phi}e^{-i\mathrm{k}z\cos\zeta}$. To determine the coefficients A_n and B_n we use the orthogonality of the vector harmonics, which requires that we evaluate the integrals

$$g_n^{(1)} = \int_0^{2\pi} e^{-i(n\phi + \rho\cos\phi)}\, d\phi,$$

$$g_n^{(2)} = \int_0^{2\pi} e^{-i(n\phi + \rho\cos\phi)}\cos\phi\, d\phi,$$

$$g_n^{(3)} = \int_0^{2\pi} e^{-i(n\phi + \rho\cos\phi)}\sin\phi\, d\phi,$$

where $\rho = kr\sin\zeta$. From the integral representation of the Bessel function $J_n(\rho)$, which is real for real ρ,

$$J_n(\rho) = \frac{i^{-n}}{2\pi}\int_0^{2\pi} e^{i(n\phi+\rho\cos\phi)}\,d\phi,$$

it immediately follows that $\mathcal{J}_n^{(1)} = 2\pi(-i)^n J_n(\rho)$; $\mathcal{J}_n^{(2)} = 2\pi i(-i)^n J_n'(\rho)$ is obtained by differentiating $\mathcal{J}_n^{(1)}$ with respect to ρ. The third integral may be written

$$2i\mathcal{J}_n^{(3)} = \mathcal{J}_{n-1}^{(1)} - \mathcal{J}_{n+1}^{(1)},$$

and if we use the identity

$$\frac{2nZ_n}{\rho} = Z_{n-1} + Z_{n+1},$$

it follows that $\mathcal{J}_n^{(3)} = 2\pi(-i)^n J_n(\rho)n/\rho$. All that is required now is a good bit of patience to show that

$$A_n = 0, \qquad B_n = \frac{E_0(-i)^n}{k\sin\zeta};$$

therefore, the expansion of the incident electromagnetic field is

$$\mathbf{E}_i = \sum_{n=-\infty}^{\infty} E_n\mathbf{N}_n^{(1)}, \qquad \mathbf{H}_i = \frac{-ik}{\omega\mu}\sum_{n=-\infty}^{\infty} E_n\mathbf{M}_n^{(1)},$$

where $E_n = E_0(-i)^n/k\sin\zeta$.

In order to satisfy the continuity conditions (3.7) for all values of z on the boundary of the cylinder, the separation constant h in the wave functions that generate the vector harmonics of the field inside the cylinder must also be $-k\cos\zeta$; finiteness at the origin requires that J_n is the appropriate Bessel function. Thus the generating functions for the internal field $(\mathbf{E}_1, \mathbf{H}_1)$ are $J_n(kr\sqrt{m^2 - \cos^2\zeta})e^{in\phi}e^{-ikz\cos\zeta}$, where m is the refractive index of the cylinder relative to that of the surrounding medium. The corresponding expansions are

$$\mathbf{E}_1 = \sum_{n=-\infty}^{\infty} E_n\left[g_n\mathbf{M}_n^{(1)} + f_n\mathbf{N}_n^{(1)}\right],$$

$$\mathbf{H}_1 = \frac{-ik_1}{\omega\mu_1}\sum_{n=-\infty}^{\infty} E_n\left[g_n\mathbf{N}_n^{(1)} + f_n\mathbf{M}_n^{(1)}\right].$$

The Hankel functions $H_n^{(1)} = J_n + iY_n$ and $H_n^{(2)} = J_n - iY_n$ are also linearly

independent solutions to (8.28); they are given asymptotically by (4.41):

$$H_n^{(1)}(\rho) \sim \sqrt{\frac{2}{\pi\rho}}\, e^{i\rho}(-i)^n e^{-i\pi/4}, \qquad |\rho| \gg n^2.$$

$$H_n^{(2)}(\rho) \sim \sqrt{\frac{2}{\pi\rho}}\, e^{-i\rho} i^n e^{i\pi/4},$$

Therefore, if the scattered field $(\mathbf{E}_s, \mathbf{H}_s)$ is to be an outgoing wave at large distances from the cylinder, the generating functions in the expansions

$$\mathbf{E}_s = -\sum_{n=-\infty}^{\infty} E_n\left[b_{n\mathrm{I}}\mathbf{N}_n^{(3)} + ia_{n\mathrm{I}}\mathbf{M}_n^{(3)}\right],$$

$$\mathbf{H}_s = \frac{i\mathrm{k}}{\omega\mu}\sum_{n=-\infty}^{\infty} E_n\left[b_{n\mathrm{I}}\mathbf{M}_n^{(3)} + ia_{n\mathrm{I}}\mathbf{N}_n^{(3)}\right],$$

must be $H_n^{(1)}(\mathrm{k}r\sin\zeta)e^{in\phi}e^{-i\mathrm{k}z\cos\zeta}$.

If we apply the conditions (3.7) at $r = a$, we obtain four equations in the four expansion coefficients, which can be solved for the coefficients $a_{n\mathrm{I}}$, $b_{n\mathrm{I}}$ of the scattered field:

$$a_{n\mathrm{I}} = \frac{C_nV_n - B_nD_n}{W_nV_n + iD_n^2}, \qquad b_{n\mathrm{I}} = \frac{W_nB_n + iD_nC_n}{W_nV_n + iD_n^2},$$

$$D_n = n\cos\zeta\,\eta J_n(\eta)H_n^{(1)}(\xi)\left(\frac{\xi^2}{\eta^2} - 1\right),$$

$$B_n = \xi\left[m^2\xi J_n'(\eta)J_n(\xi) - \eta J_n(\eta)J_n'(\xi)\right],$$

$$C_n = n\cos\zeta\,\eta J_n(\eta)J_n(\xi)\left(\frac{\xi^2}{\eta^2} - 1\right), \tag{8.29}$$

$$V_n = \xi\left[m^2\xi J_n'(\eta)H_n^{(1)}(\xi) - \eta J_n(\eta)H_n^{(1)\prime}(\xi)\right],$$

$$W_n = i\xi\left[\eta J_n(\eta)H_n^{(1)\prime}(\xi) - \xi J_n'(\eta)H_n^{(1)}(\xi)\right],$$

where $\xi = x\sin\zeta$, $\eta = x\sqrt{m^2 - \cos^2\zeta}$, $x = \mathrm{k}a$, and we have taken $\mu = \mu_1$. It follows from the relations $J_{-n} = (-1)^nJ_n$ and $Y_{-n} = (-1)^nY_n$ that

$$a_{-n\mathrm{I}} = -a_{n\mathrm{I}}, \qquad b_{-n\mathrm{I}} = b_{n\mathrm{I}}, \qquad a_{0\mathrm{I}} = 0.$$

When the incident light is normal to the cylinder axis ($\zeta = 90°$), $a_{n\mathrm{I}}$ vanishes

and

$$b_{n\mathrm{I}}(\zeta = 90°) = b_n = \frac{J_n(mx)J_n'(x) - mJ_n'(mx)J_n(x)}{J_n(mx)H_n^{(1)\prime}(x) - mJ_n'(mx)H_n^{(1)}(x)}. \tag{8.30}$$

Case II. Incident Electric Field Perpendicular to the xz Plane. The expansion of the incident electric field $\mathbf{E}_i = E_0\hat{\mathbf{e}}_y e^{-ik(r\sin\zeta\cos\phi + z\cos\zeta)}$ is

$$\mathbf{E}_i = -i\sum_{n=-\infty}^{\infty} E_n\mathbf{M}_n^{(1)},$$

the curl of which gives the incident magnetic field. The coefficients of the scattered field

$$\mathbf{E}_s = \sum_{n=-\infty}^{\infty} E_n\left[ia_{n\mathrm{II}}\mathbf{M}_n^{(3)} + b_{n\mathrm{II}}\mathbf{N}_n^{(3)}\right],$$

can be written in the form

$$a_{n\mathrm{II}} = -\frac{A_nV_n - iC_nD_n}{W_nV_n + iD_n^2}, \qquad b_{n\mathrm{II}} = -i\frac{C_nW_n + A_nD_n}{W_nV_n + iD_n^2}, \tag{8.31}$$

where D_n, C_n, and so on, were defined in the preceding section and

$$A_n = i\xi\left[\xi J_n'(\eta)J_n(\xi) - \eta J_n(\eta)J_n'(\xi)\right].$$

It follows from the properties of the Bessel functions that

$$a_{-n\mathrm{II}} = a_{n\mathrm{II}}, \qquad b_{-n\mathrm{II}} = -b_{n\mathrm{II}}, \qquad b_{0\mathrm{II}} = 0.$$

Although it is not obvious, it is not too difficult to show that

$$a_{n\mathrm{I}} = -b_{n\mathrm{II}}.$$

This was pointed out by Kerker et al. (1966). When the incident light is normal to the cylinder axis, $b_{n\mathrm{II}}$ vanishes and

$$a_{n\mathrm{II}}(\zeta = 90°) = a_n = \frac{mJ_n'(x)J_n(mx) - J_n(x)J_n'(mx)}{mJ_n(mx)H_n^{(1)\prime}(x) - J_n'(mx)H_n^{(1)}(x)}. \tag{8.32}$$

8.4.1 Asymptotic Scattered Field

At large distances from the cylinder ($kr\sin\zeta \gg 1$), the scattered field (Case I) is given asymptotically by

$$\mathbf{E}_s \sim -E_0e^{-i\pi/4}\sqrt{\frac{2}{\pi kr\sin\zeta}}\,e^{ik(r\sin\zeta - z\cos\zeta)}$$

$$\times\sum_n(-1)^n e^{in\phi}\left[a_{n\mathrm{I}}\hat{\mathbf{e}}_\phi + b_{n\mathrm{I}}(\cos\zeta\hat{\mathbf{e}}_r + \sin\zeta\hat{\mathbf{e}}_z)\right]. \tag{8.33}$$

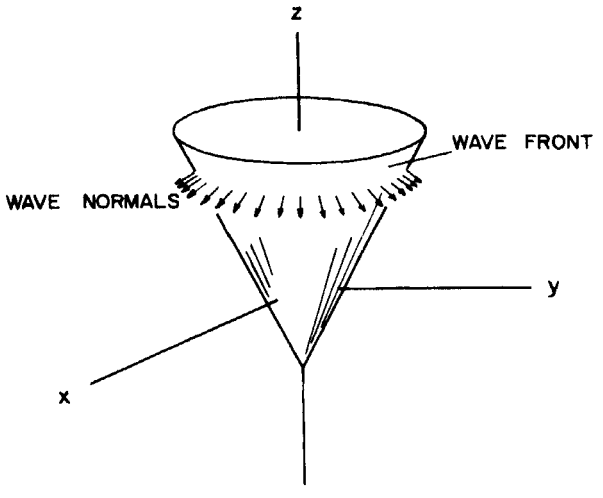

Figure 8.4 Wave front and wave normals of light scattered by an infinite cylinder.

When the incident electric field is polarized perpendicular to the xz plane (Case II), the asymptotic scattered field is given by (8.33) with $a_{n\mathrm{I}}$ replaced by $-a_{n\mathrm{II}}$ and $b_{n\mathrm{I}}$ replaced by $-b_{n\mathrm{II}}$.

The surfaces of constant phase, or *wave fronts*, of the scattered wave (8.33), the points on which satisfy

$$f(x, y, z) = r\sin\zeta - z\cos\zeta = C,$$

are *cones* of half-angle ζ and apexes at $z = -C/\cos\zeta$ (Fig. 8.4). Thus, we may visualize the propagation of the scattered wave as a cone that is sliding down the cylinder. At any point on the cone, the direction of propagation, or *wave normal* $\hat{\mathbf{e}}_s$, is

$$\hat{\mathbf{e}}_s = \nabla f = \sin\zeta\hat{\mathbf{e}}_r - \cos\zeta\hat{\mathbf{e}}_z.$$

The Poynting vector, therefore, is in the direction $\hat{\mathbf{e}}_s$. When the incident beam is normal to the cylinder axis ($\zeta = 90°$), the cone reduces to a cylinder.

A convincing and aesthetically pleasing demonstration that the light scattered by a long cylinder is a conical wave can be made by illuminating a fiber with a narrow laser beam. If a screen perpendicular to the incident beam is placed at some distance from the fiber, the resulting patterns formed on the screen will be *conic sections*. When the incident light is normal to the fiber axis, the pattern is a straight line. As ζ is decreased, a succession of *hyperbolas* are traced out, and at $\zeta = 45°$ the pattern is a *parabola*. For angles of incidence less than 45°, *ellipses* appear on the screen, the eccentricities of which decrease with decreasing ζ; as ζ approaches 0° the pattern approaches a circle. In Fig. 8.5 we show a series of photographs, taken with an oscilloscope camera, of the

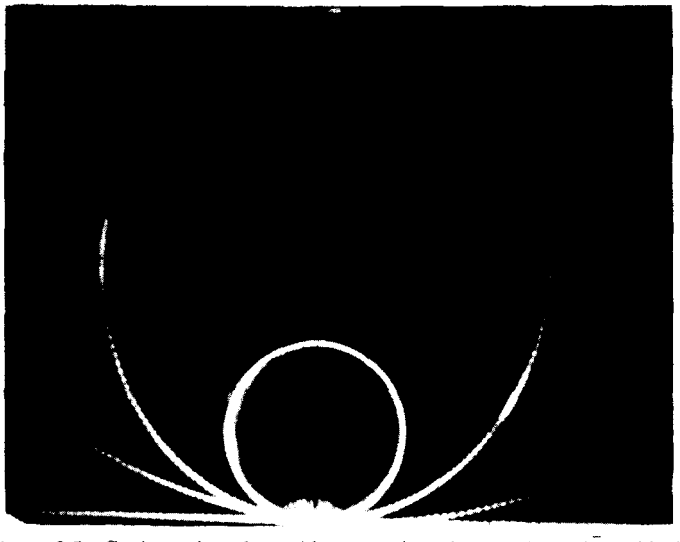

Figure 8.5 Conic sections formed by scattering of a laser beam by a thin fiber.

patterns formed on a screen when a laser beam is scattered by a thin fiber. In addition to showing the various conic sections that result from varying the angle ζ, this figure also shows some of the maxima and minima of the scattering diagram.

8.4.2 Amplitude Scattering Matrix

In Chapter 3 we derived a general expression for the amplitude scattering matrix for an arbitrary particle. An unstated assumption underlying that derivation is that the particle is confined within a bounded region, a condition that is not satisfied by an infinite cylinder. Nevertheless, we can express the field scattered by such a cylinder in a concise form by resolving the incident and scattered fields into components parallel and perpendicular to planes determined by the cylinder axis ($\hat{\mathbf{e}}_z$) and the appropriate wave normals (see Fig. 8.3). That is, we write the incident field

$$\mathbf{E}_i = \left(E_{\|i}\hat{\mathbf{e}}_{\|i} + E_{\perp i}\hat{\mathbf{e}}_{\perp i}\right)e^{i\mathbf{k}\cdot\mathbf{x}},$$

$$\hat{\mathbf{e}}_{\|i} = \sin\zeta\hat{\mathbf{e}}_z - \cos\zeta\hat{\mathbf{e}}_x, \qquad \hat{\mathbf{e}}_{\perp i} = -\hat{\mathbf{e}}_y, \qquad \hat{\mathbf{e}}_{\perp i} \times \hat{\mathbf{e}}_{\|i} = \hat{\mathbf{e}}_i.$$

The scattered field is the sum of components parallel and perpendicular to the

plane ϕ = constant:

$$\mathbf{E}_s = E_{\|s}\hat{\mathbf{e}}_{\|s} + E_{\perp s}\hat{\mathbf{e}}_{\perp s},$$

$$\hat{\mathbf{e}}_{\|s} = \cos\zeta\hat{\mathbf{e}}_r + \sin\zeta\hat{\mathbf{e}}_z, \qquad \hat{\mathbf{e}}_{\perp s} = \hat{\mathbf{e}}_\phi, \qquad \hat{\mathbf{e}}_{\perp s} \times \hat{\mathbf{e}}_{\|s} = \hat{\mathbf{e}}_s.$$

We may now write the relation between incident and scattered fields in matrix form:

$$\begin{pmatrix} E_{\|s} \\ E_{\perp s} \end{pmatrix} = e^{i3\pi/4}\sqrt{\frac{2}{\pi kr\sin\zeta}}\, e^{ik(r\sin\zeta - z\cos\zeta)} \begin{pmatrix} T_1 & T_4 \\ T_3 & T_2 \end{pmatrix} \begin{pmatrix} E_{\|i} \\ E_{\perp i} \end{pmatrix},$$

$$T_1 = \sum_{-\infty}^{\infty} b_{n\mathrm{I}} e^{-in\Theta} = b_{0\mathrm{I}} + 2\sum_{n=1}^{\infty} b_{n\mathrm{I}}\cos(n\Theta),$$

$$T_2 = \sum_{-\infty}^{\infty} a_{n\mathrm{II}} e^{-in\Theta} = a_{0\mathrm{II}} + 2\sum_{n=1}^{\infty} a_{n\mathrm{II}}\cos(n\Theta), \tag{8.34}$$

$$T_3 = \sum_{-\infty}^{\infty} a_{n\mathrm{I}} e^{-in\Theta} = -2i\sum_{n=1}^{\infty} a_{n\mathrm{I}}\sin(n\Theta),$$

$$T_4 = \sum_{-\infty}^{\infty} b_{n\mathrm{II}} e^{-in\Theta} = -2i\sum_{n=1}^{\infty} b_{n\mathrm{II}}\sin(n\Theta) = -T_3,$$

where we have transformed the angle variable ϕ to $\Theta = \pi - \phi$.

Unlike the amplitude scattering matrix for a sphere (Chapter 4), the off-diagonal elements of the amplitude scattering matrix for a cylinder are, in general, nonzero. Thus, if the incident light is polarized *parallel* (perpendicular) to the xz plane, the scattered light has a component *perpendicular* (parallel) to the plane determined by the cylinder axis and the scattering direction $\hat{\mathbf{e}}_s$. However, symmetry requires that T_3 and T_4 vanish when $\hat{\mathbf{e}}_s$ lies in the forward scattering plane ($\Theta = 0°$) and the backward scattering plane ($\Theta = 180°$). When the incident light is normal to the cylinder axis, T_3 and T_4 are identically zero for all Θ.

8.4.3 Cross Sections

Although we have repeatedly referred to an "infinite" cylinder, it is clear that no such cylinder exists except as an idealization. So what we really have in mind is a cylinder long compared with its diameter. Later in this section we shall try to acquire some insight into how long a cylinder must be before it is effectively infinite by considering scattering in the diffraction theory approximation.

The scattering and absorption cross sections of an infinite cylinder are, of course, infinite; however, the light scattered and absorbed per unit length of such a cylinder is finite. If we ignore end effects the ratio $W_s/L(W_a/L)$ for a finite cylinder of length L can be approximated by the amount of light scattered (absorbed) per unit length of an infinite cylinder; this approximation will be increasingly better the greater the ratio of cylinder length to diameter.

In a manner similar to that in Section 3.4, where we considered cross sections of finite particles, we can calculate cross sections *per unit length* of an infinite cylinder by constructing an imaginary closed concentric surface A of length L and radius R (Fig. 8.6). The rate W_a at which energy is absorbed within this surface is

$$W_a = -\int_A \mathbf{S} \cdot \hat{\mathbf{n}}\, dA = W_{\text{ext}} - W_s,$$

where $\mathbf{S}$ is the Poynting vector. There is no net contribution to W_a from the ends of A; therefore,

$$W_s = RL\int_0^{2\pi} (\mathbf{S}_s)_r\, d\phi, \qquad W_{\text{ext}} = RL\int_0^{2\pi} (\mathbf{S}_{\text{ext}})_r\, d\phi, \tag{8.35}$$

where $(\mathbf{S}_s)_r$ and $(\mathbf{S}_{\text{ext}})_r$ are the radial components of

$$\mathbf{S}_s = \tfrac{1}{2}\,\text{Re}\{\mathbf{E}_s \times \mathbf{H}_s^*\}, \qquad S_{\text{ext}} = \tfrac{1}{2}\,\text{Re}\{\mathbf{E}_i \times \mathbf{H}_s^* + \mathbf{E}_s \times \mathbf{H}_i^*\}.$$

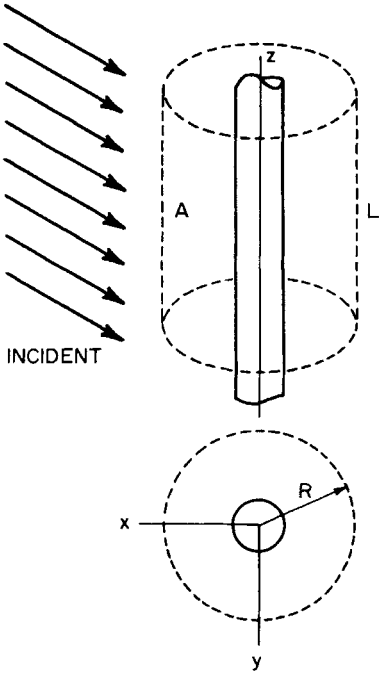

Figure 8.6 Surface of integration (dashed lines).

Let us consider the incident electric field parallel to the xz plane (Case I). If the series expansions of the incident and scattered fields are substituted into the expressions for the vectors $\mathbf{S}_s$ and $\mathbf{S}_{ext}$, then after performing the required integrations in (8.35) we obtain the efficiencies $Q_{sca,I}$ and $Q_{ext,I}$ for scattering and extinction:

$$Q_{sca,I} = \frac{W_{s,I}}{2aLI_i} = \frac{2}{x}\left[|b_{0I}|^2 + 2\sum_{n=1}^{\infty}\left(|b_{nI}|^2 + |a_{nI}|^2\right)\right],$$

$$Q_{ext,I} = \frac{W_{ext,I}}{2aLI_i} = \frac{2}{x}\,\mathrm{Re}\left\{b_{0I} + 2\sum_{n=1}^{\infty} b_{nI}\right\}. \tag{8.36}$$

Note that

$$Q_{ext,I} = \frac{2}{x}\,\mathrm{Re}\{T_1(\Theta = 0°)\},$$

which is the *optical theorem* for an infinite cylinder (see Section 3.4).

In a similar manner we obtain the scattering and extinction efficiencies when the incident electric field is polarized perpendicular to the xz plane (Case II):

$$Q_{sca,II} = \frac{2}{x}\left[|a_{0II}|^2 + 2\sum_{n=1}^{\infty}\left(|a_{nII}|^2 + |b_{nII}|^2\right)\right],$$

$$Q_{ext,II} = \frac{2}{x}\,\mathrm{Re}\left\{a_{0II} + 2\sum_{n=1}^{\infty} a_{nII}\right\} = \frac{2}{x}\,\mathrm{Re}\{T_2(\Theta = 0°)\}. \tag{8.37}$$

If the incident light is *unpolarized*, the efficiencies are

$$Q_{sca} = \tfrac{1}{2}(Q_{sca,I} + Q_{sca,II}), \qquad Q_{ext} = \tfrac{1}{2}(Q_{ext,I} + Q_{ext,II}).$$

8.4.4 Normally Incident Light

If the incident light is normal to the cylinder axis the scattering coefficients have their simplest form. However, the coefficients (8.30) and (8.32) are not in the form most suitable for computations. If we introduce the logarithmic derivative

$$D_n(\rho) = \frac{J_n'(\rho)}{J_n(\rho)}$$

and use the recurrence relation

$$Z_n'(x) = Z_{n-1}(x) - \frac{n}{x}Z_n(x),$$

where Z_n is any Bessel function, the scattering coefficients may be written

$$a_n = \frac{[D_n(mx)/m + n/x]J_n(x) - J_{n-1}(x)}{[D_n(mx)/m + n/x]H_n^{(1)}(x) - H_{n-1}^{(1)}(x)},$$

$$b_n = \frac{[mD_n(mx) + n/x]J_n(x) - J_{n-1}(x)}{[mD_n(mx) + n/x]H_n^{(1)}(x) - H_{n-1}^{(1)}(x)}. \tag{8.38}$$

The logarithmic derivative satisfies the recurrence relation

$$D_{n-1}(z) = \frac{n-1}{z} - \frac{1}{(n/z) + D_n(z)}. \tag{8.39}$$

A computer program for calculating the scattering coefficients (8.38) and the corresponding cross sections and scattering matrix elements is described in Appendix C; all the examples in this section were obtained with this program.

The amplitude scattering matrix for a normally illuminated cylinder is diagonal:

$$\begin{pmatrix} E_{\parallel s} \\ E_{\perp s} \end{pmatrix} = e^{i3\pi/4}\sqrt{\frac{2}{\pi kr}}\, e^{ikr}\begin{pmatrix} T_1 & 0 \\ 0 & T_2 \end{pmatrix}\begin{pmatrix} E_{\parallel i} \\ E_{\perp i} \end{pmatrix}. \tag{8.40}$$

Note that the surfaces of constant phase of the scattered wave are cylinders. Thus, the light scattered by a cylinder long compared with its diameter will not be seen by a suitably collimated detector unless it "looks" in a direction perpendicular to the cylinder axis. Many examples of this are commonly encountered, most of which probably go unnoticed. For example, randomly oriented scratches on a car windshield form a circular pattern when illuminated by the headlights of an oncoming car; dust on the windshield, on the other hand, forms no such obvious pattern. The scratches are sufficiently long compared with their lateral dimensions that they may be considered to be infinite cylinders; thus, only those scratches perpendicular to a line from the eye to a scratch will scatter light into the eye, and such scratches lie on circles centered on the line of sight. If a point source is viewed through a fibrous material, one may also see circular patterns: Christmas tree lights embedded in wisps of "angel's hair" are seen to be surrounded by haloes of scattered light; steel wool will yield the same effect.

The scattering matrix corresponding to (8.40)

$$\begin{pmatrix} I_s \\ Q_s \\ U_s \\ V_s \end{pmatrix} = \frac{2}{\pi k r} \begin{pmatrix} T_{11} & T_{12} & 0 & 0 \\ T_{12} & T_{11} & 0 & 0 \\ 0 & 0 & T_{33} & T_{34} \\ 0 & 0 & -T_{34} & T_{33} \end{pmatrix} \begin{pmatrix} I_i \\ Q_i \\ U_i \\ V_i \end{pmatrix}$$

$$T_{11} = \tfrac{1}{2}\left(|T_1|^2 + |T_2|^2\right), \qquad T_{12} = \tfrac{1}{2}\left(|T_1|^2 - |T_2|^2\right),$$

$$T_{33} = \mathrm{Re}\{T_1 T_2^*\}, \qquad T_{34} = \mathrm{Im}\{T_1 T_2^*\},$$

has the same form as that for a sphere (4.77). However, there are appreciable differences between scattering by a sphere and by a normally illuminated cylinder. For example, the ratio $P = T_{12}/T_{11}$, which is analogous to (4.78), does not necessarily vanish in the forward (or backward) direction. Thus, if the incident light is unpolarized, the forward scattered light will, in general, be partially polarized. Scattering and extinction cross sections for a nonactive sphere are independent of the state of polarization of the incident light; however, these quantities for a cylinder may be quite different for different polarizations. This is illustrated in Fig. 8.7, where the scattering cross sections

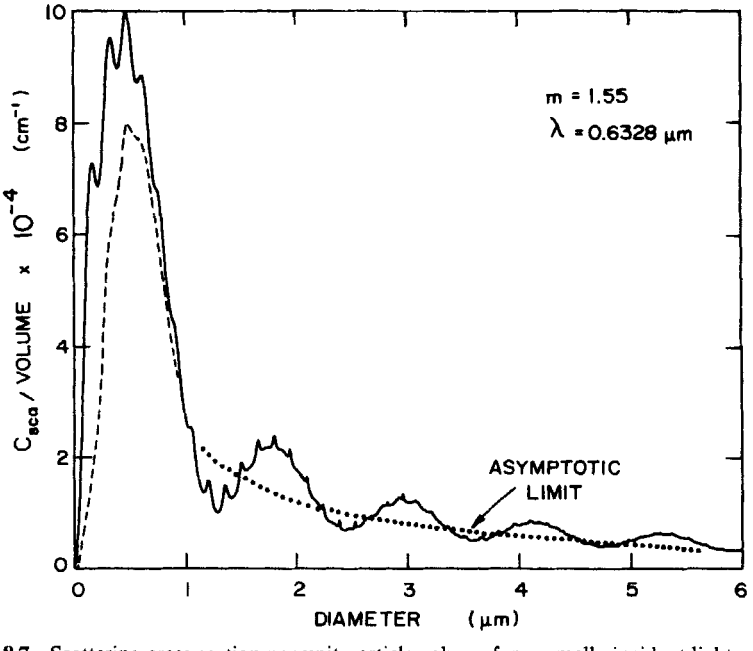

Figure 8.7 Scattering cross section per unit particle volume for normally incident light polarized parallel (——) and perpendicular (------) to the axis of an infinite cylinder in air.

per unit particle volume for incident light polarized parallel and perpendicular to the cylinder axis are plotted as functions of diameter. The cylinder is in air and is taken to be nonabsorbing with a refractive index of 1.55; this corresponds approximately to many silicates at visible wavelengths. The wavelength 0.6328 μm is that of the He–Ne laser. In Section 4.4 we showed that the extinction cross section of an object large compared with the wavelength is twice its geometrical cross section G. Therefore, the scattering cross section per unit volume of a nonabsorbing cylinder asymptotically approaches the limiting value

$$\frac{C_{sca}}{v} \sim \frac{2G}{v} = \frac{4}{\pi a} \tag{8.41}$$

independently of the state of polarization of the incident light; the limit (8.41) is also plotted in Fig. 8.7. This figure deserves careful study, for there is much to be learned from it. If the size parameter is greater than about 5, there is essentially no difference between scattering of incident light polarized parallel or perpendicular to the cylinder axis. However, for smaller size parameters, there can be appreciable difference; the maximum occurs for $x \simeq 1$. Note also that the scattering cross section per unit particle volume has its greatest value for $x = 2.5$, which corresponds to a particle diameter of about 0.5 μm; thus,

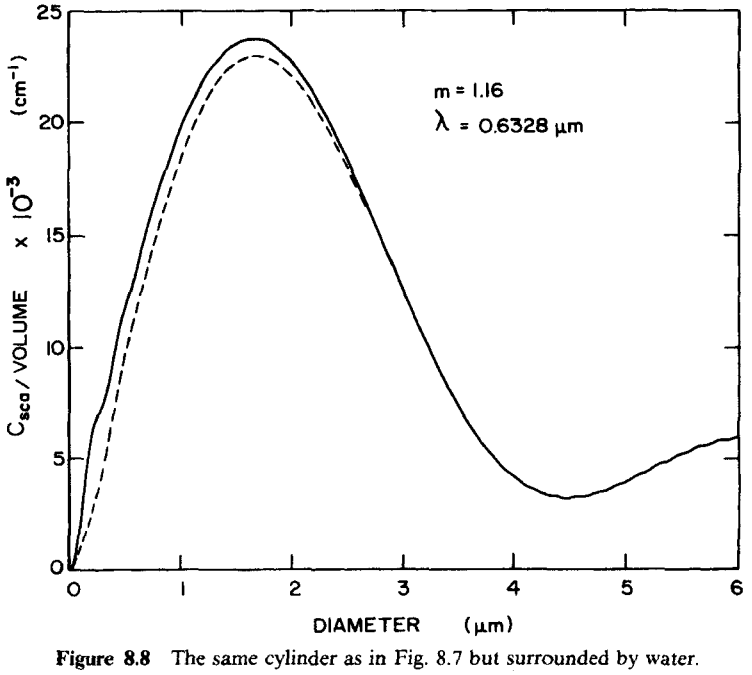

Figure 8.8 The same cylinder as in Fig. 8.7 but surrounded by water.

cylindrical particles of this size are the most effective at scattering light from the beam. The consequences of changing the surrounding medium from air to water are striking; this is shown in Fig. 8.8. Regardless of the particle diameter, the scattering cross section is only weakly dependent upon the polarization state of the incident light. The shapes of the two sets of curves are markedly different: when the cylinder is in water the ripples disappear and the diameter at which C_{sca}/v is a maximum shifts from 0.5 μm to about 1.1 μm.

8.4.5 Small-Particle Limit

If x and $|m|x$ are sufficiently small, then the scattering coefficients a_0 and b_0 are approximately

$$a_0 \simeq \frac{-i\pi x^4(m^2-1)}{32}, \qquad b_0 \simeq \frac{-i\pi x^2(m^2-1)}{4}. \tag{8.42}$$

To obtain (8.42) we substituted the following expressions for the Bessel functions and their derivatives

$$J_0(z) \simeq 1 - \frac{z^2}{4}, \qquad J_0'(z) \simeq -\frac{z}{2} + \frac{z^3}{16},$$
$$Y_0(z) \simeq \frac{2}{\pi}\log\left(\frac{z}{2}\right), \qquad Y_0'(z) \simeq \frac{2}{\pi z}, \qquad |z| \ll 1$$

in (8.30) and (8.32) and retained the terms of smallest degree in x. Similarly, if we use

$$J_1(z) \simeq \frac{z}{2} - \frac{z^3}{16}, \qquad J_1'(z) \simeq \frac{1}{2} - \frac{3z^2}{16},$$
$$Y_1(z) \simeq -\frac{2}{\pi z}, \qquad Y_1'(z) \simeq \frac{2}{\pi z^2}, \qquad |z| \ll 1$$

we obtain the following approximations for a_1 and b_1:

$$a_1 \simeq \frac{-i\pi x^2}{4}\frac{m^2-1}{m^2+1}, \qquad b_1 \simeq \frac{-i\pi x^4(m^2-1)}{32}.$$

The amplitude scattering matrix elements correct to terms of order x^2 are

$$T_1 = b_0, \qquad T_2 = 2a_1\cos\Theta.$$

Thus, the degree of polarization of scattered light, given unpolarized incident

light, is

$$P = \frac{|m^2 + 1|^2 - 4\cos^2\Theta}{|m^2 + 1|^2 + 4\cos^2\Theta}.$$

At $\Theta = 90°$, therefore, the scattered light is 100% polarized along the cylinder axis.

8.4.6 Anisotropic Cylinder

Scattering problems in which the particle is composed of an anisotropic material are generally intractable. One of the few exceptions to this generalization is a normally illuminated cylinder composed of a uniaxial material, where the cylinder axis coincides with the optic axis. That is, if the constitutive relation connecting **D** and **E** is

$$\begin{pmatrix} D_x \\ D_y \\ D_z \end{pmatrix} = \begin{pmatrix} \varepsilon_\perp & 0 & 0 \\ 0 & \varepsilon_\perp & 0 \\ 0 & 0 & \varepsilon_\parallel \end{pmatrix} \begin{pmatrix} E_x \\ E_y \\ E_z \end{pmatrix},$$

where the z axis is parallel to the cylinder axis, then the scattering problem has an exact solution. It is not difficult to show that the scattering coefficients a_n and b_n are of the form (8.32) and (8.30):

$$a_n = a_n(x, m_\perp), \qquad b_n = b_n(x, m_\parallel),$$

where $m_\perp$ and $m_\parallel$ are the complex refractive indices corresponding to the principal values $\varepsilon_\perp$ and $\varepsilon_\parallel$ of the permittivity tensor. Thus, if the incident light is polarized parallel to the cylinder axis, the cylinder scatters and absorbs light as if it were isotropic with permittivity $\varepsilon_\parallel$; on the other hand, incident light polarized perpendicular to the cylinder axis is oblivious to the permittivity along the axis and responds only to $\varepsilon_\perp$.

8.4.7 Diffraction Theory

Scattering by a cylinder of *finite* length cannot be treated exactly by constructing separable solutions to the scalar wave equation and expanding the various fields in the corresponding vector harmonics, a method that has to this point served us quite well. A finite cylinder has an edge, which is the bane of this scattering problem. However, by considering the diffraction theory approximation, we can acquire some insight into scattering by a finite cylinder. According to this theory, which was discussed in Section 4.4, an opaque cylinder, an opaque rectangular obstacle, and a rectangular aperture in an opaque screen, all with the same projected cross sectional area, scatter light in the same

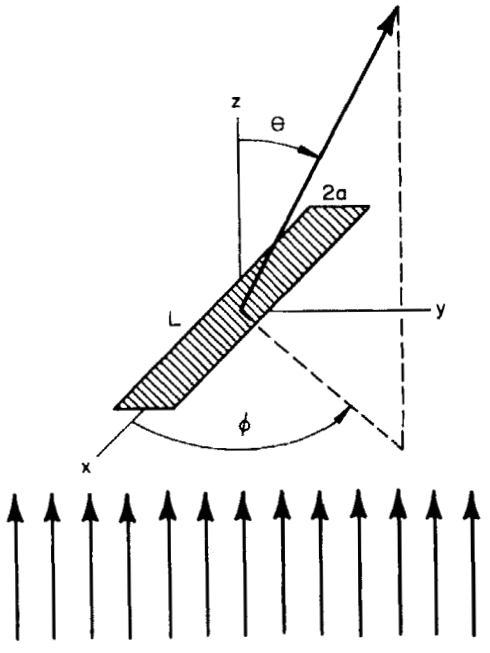

Figure 8.9 An opaque rectangular obstacle illuminated by a plane wave.

manner independently of the polarization of the incident light. Let us therefore consider scattering (diffraction) by the opaque obstacle shown in Fig. 8.9. The amplitude of the scattered wave is, from (4.70), given by

$$S(\theta, \phi) = \frac{\mathrm{k}^2(1 + \cos\theta)}{4\pi} \int_{-a}^{a} \int_{-L/2}^{L/2} e^{-i\mathrm{k}\sin\theta(\xi\cos\phi + \eta\sin\phi)} d\xi\, d\eta,$$

which can be integrated readily to yield

$$S(\theta, \phi) = \frac{(1 + \cos\theta)}{\pi} \frac{x\sin(x\sin\theta\sin\phi)}{x\sin\theta\sin\phi} \frac{xR\sin(xR\sin\theta\cos\phi)}{xR\sin\theta\cos\phi},$$

where R is the ratio of length to diameter ($L/2a$) and $x = \mathrm{k}a$. The diffraction cross section is equal to the geometrical cross section G:

$$\int_0^{2\pi} \int_0^{\pi} \frac{|S(\theta, \phi)|^2}{\mathrm{k}^2} \sin\theta\, d\theta\, d\phi = 2aL = 4a^2R.$$

The phase function $p(\theta, \phi) = |S(\theta, \phi)|^2/4x^2R$, which is the fraction of the total scattered light that is scattered into a unit solid angle about a given

direction (θ, ϕ), has its greatest value in the forward direction:

$$p(0°) = \frac{x^2R}{\pi^2} = \frac{k^2aL}{2\pi^2}.$$

Therefore, the greater the dimensions of the particle (radius or length), the more the scattered light is concentrated about the forward direction.

It is instructive to consider how p varies with scattering angle θ for the two azimuthal angles 0° and 90°. For scattering directions in a plane *perpendicular* to the cylinder axis the phase function $p(\theta, 90°)$ is $p_e(\theta, 90°)\sin^2(x\sin\theta)$, where the *envelope*

$$p_e(\theta, 90°) = \left(\frac{1 + \cos\theta}{2}\right)^2 \frac{p(0°)}{x^2\sin^2\theta}$$

is modulated by the rapidly oscillating function $\sin^2(x\sin\theta)$. Similarly, for directions in a plane *parallel* to the cylinder axis, we have $p(\theta, 0°) = p_e(\theta, 0°)\sin^2(xR\sin\theta)$, where

$$p_e(\theta, 0°) = \left(\frac{1 + \cos\theta}{2}\right)^2 \frac{p(0°)}{x^2R^2\sin^2\theta}.$$

The ratio of the envelopes is

$$\frac{p_e(\theta, 90°)}{p_e(\theta, 0°)} = R^2. \tag{8.43}$$

Equation (8.43) provides us with an approximate criterion, subject to the limitations of diffraction theory, for when a finite cylinder may be regarded as effectively infinite: if $R > 10$, say, there will be comparatively little light scattered in directions other than those in a plane perpendicular to the cylinder axis. The greater is R, the more the scattered light is concentrated in this plane; in the limit of indefinitely large R, no light is scattered in directions other than in this plane. We may show this as follows. The phase function may be written in the form $p(\theta, \phi) = G(\theta, \phi)F(\theta, \phi)$, where

$$G(\theta, \phi) = \left[\frac{1 + \cos\theta}{\pi} \frac{x\sin(x\sin\theta\sin\phi)}{x\sin\theta\sin\phi}\right]^2,$$

$$F(\theta, \phi) = \frac{R}{4}\left[\frac{\sin(xR\sin\theta\cos\phi)}{xR\sin\theta\cos\phi}\right]^2.$$

For all azimuthal angles except 90° and 270°

$$\lim_{R\to\infty} F(\theta, \phi) = 0 \qquad (\theta \neq 0).$$

However, the integrals

$$\int_0^{\pi} F(\theta, \phi)\, d\phi, \qquad \int_{\pi}^{2\pi} F(\theta, \phi)\, d\phi,$$

are nonzero for all R and have the limiting value $\pi/4x \sin\theta$ as R approaches infinity. Therefore,

$$\lim_{R \to \infty} F(\theta, \phi) = \frac{\pi}{4x \sin\theta}\left[\delta\left(\phi - \frac{\pi}{2}\right) + \delta\left(\phi - \frac{3\pi}{2}\right)\right],$$

where δ is the Dirac delta function. If we denote the phase function for indefinitely large R by $\bar{p}$, then

$$\int_0^{2\pi}\int_0^{\pi} \bar{p}(\theta, \phi)\sin\theta\, d\theta\, d\phi = \frac{\pi}{2x}\int_0^{\pi}\left[\frac{1 + \cos\theta}{\pi}\,\frac{x\sin(x\sin\theta)}{x\sin\theta}\right]^2 d\theta = 1.$$

We need consider only scattering directions in the plane $\phi = \pi/2$ (or $\phi = 3\pi/2$) because $\bar{p}$ vanishes outside this plane; we also have $\Theta = \theta$ when $\phi = \pi/2$ and $\Theta = -\theta$ when $\phi = 3\pi/2$, where $\Theta = 0$ is the forward direction. Thus, we may take the phase function for scattering by an infinite cylinder in the diffraction theory approximation to be

$$p(\Theta) = \frac{\pi}{4x}\left[\frac{1 + \cos\Theta}{\pi}\,\frac{x\sin(x\sin\Theta)}{x\sin\Theta}\right]^2, \tag{8.44}$$

which is normalized:

$$\int_{-\pi}^{\pi} p(\Theta)\, d\Theta = 1.$$

The phase function (8.44) vanishes in the backward direction ($\Theta = \pi$) and at those angles for which $\sin\Theta = n\pi/x$, where n is an integer. This gives us a means for estimating the diameter of cylinders sufficiently large that diffraction theory is a good approximation: because $|\sin\Theta| \leqslant 1$, the diameter d is

$$d \simeq \lambda n_{\min}, \tag{8.45}$$

where $n_{\min}$ is the number of minima in the phase function (8.44) between 0 and 90°. Diffraction theory should be at its best for a large opaque cylinder. An opaque particle is one that does not reflect incident light and that absorbs all transmitted light. This is an idealization: no such cylinder exists (i.e., there are no values of m and x such that these criteria are strictly satisfied). But we can conjure up an approximately opaque cylinder by taking the real part of its refractive index to be that of the surrounding medium; therefore, the reflectance at normal incidence is, from (2.58), $k^2/(4 + k^2)$. Thus, we want k to be as small as possible subject to the constraint that $kx > 1$. In Fig. 8.10 we show the phase function calculated from the exact theory for a cylinder with $x = 20$

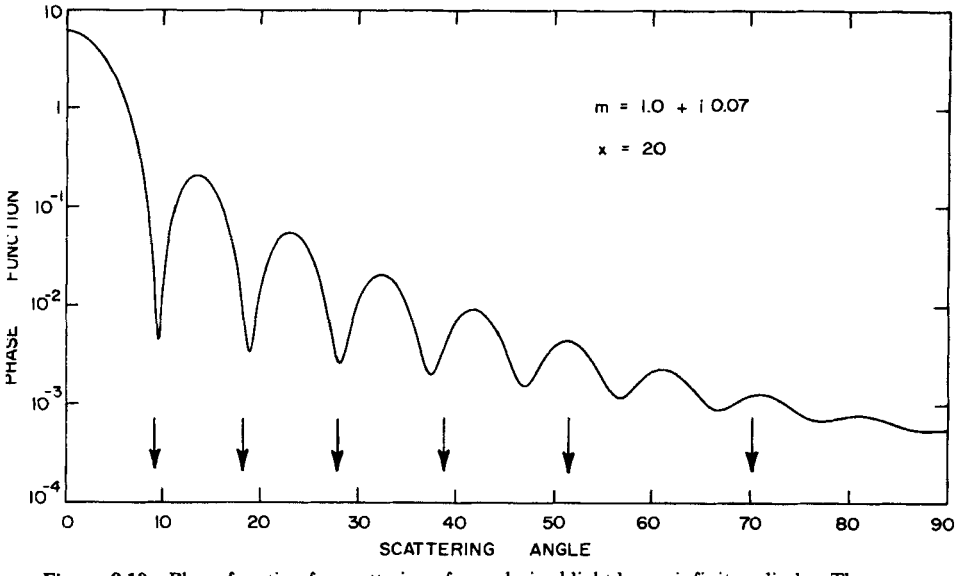

Figure 8.10 Phase function for scattering of unpolarized light by an infinite cylinder. The arrows indicate minima according to diffraction theory.

and $m = 1.0 + i0.07$; the incident light is unpolarized. Also shown are the minima in the diffraction theory phase function (8.44). The positions of the first few minima of the exact phase function are predicted quite well by diffraction theory. As the scattering angle increases, however, diffraction theory becomes an increasingly poorer approximation.

8.5 INHOMOGENEOUS PARTICLES: AVERAGE DIELECTRIC FUNCTION

Although inhomogeneous particles exist—in planetary atmospheres, for example, where particles of different composition are continually coagulating—little attention has been given to absorption and scattering by such particles except those that are regularly inhomogeneous—coated spheres, for example (Section 8.1). But we would not be tempted to recast the problem of scattering by a coated sphere in the form of scattering by an equivalent homogeneous sphere with an average, or effective, dielectric function obtained by combining somehow the dielectric functions of core and coating. For although our prescription might give good results for one size at a particular wavelength, it would not do so for other sizes and wavelengths; we would be faced with the task of continuously modifying the prescription to force the scattering and absorbing properties of the equivalent homogeneous particle into congruence with those of the inhomogeneous particle. Clearly, therefore, some kind of statistical irregularity on an appropriate scale is a necessary concomitant of a well-defined average dielectric function of an inhomogeneous medium.

The notion of homogeneity is not absolute: all substances are inhomogeneous upon sufficiently close inspection. Thus, the description of the interaction of an electromagnetic wave with *any* medium by means of a spatially uniform dielectric function is ultimately statistical, and its validity requires that the constituents—whatever their nature—be small compared with the wavelength. It is for this reason that the optical properties of media usually considered to be homogeneous—pure liquids, for example—are adequately described to first approximation by a dielectric function. There is no sharp distinction between such molecular media and those composed of small particles each of which contains sufficiently many molecules that they can be individually assigned a bulk dielectric function: we may consider the particles to be giant "molecules" with polarizabilities determined by their composition and shape.

It is not easy, however, to determine the average dielectric function of an inhomogeneous medium given the properties of its constituents: the interactions among them lead to problems which are insoluble except by approximate methods. Each type of approximation leads to a different dielectric function. As a consequence, there is a bewildering array of choices in the scientific literature, all of which are at least superficially different; moreover, there are apparently conflicting claims about the relative merits and ranges of validity of the various theories. Perhaps the Maxwell Garnett theory has the greatest following. In the following paragraphs we generalize the Maxwell Garnett theory, explore some of its properties, and discuss some experimental data on scattering by inhomogeneous particles.

We take as our model of an inhomogeneous medium a two-component mixture composed of *inclusions* embedded in an otherwise homogeneous *matrix*, where ϵ and ϵ_m are their respective dielectric functions. The inclusions are identical in composition but may be different in volume, shape, and orientation; we shall restrict ourselves, however, to ellipsoidal inclusions. The average electric field $\langle \mathbf{E} \rangle$ over a volume V surrounding the point x is defined as

$$\langle \mathbf{E}(\mathbf{x}) \rangle = \frac{1}{V} \int_V \mathbf{E}(\mathbf{x} + \boldsymbol{\xi})\, d\boldsymbol{\xi},$$

where V contains many inclusions but is otherwise arbitrary. Note that $\mathbf{E}$ itself has been obtained from a microscopic field by suitably averaging over many molecules (see, e.g., de Groot, 1969); thus, $\langle \mathbf{E} \rangle$ is an even less finely grained macroscopic field than $\mathbf{E}$. V is composed of the matrix volume and the volume of all the inclusions; therefore, we may write

$$\langle \mathbf{E}(\mathbf{x}) \rangle = (1 - f)\langle \mathbf{E}_m(\mathbf{x}) \rangle + f \sum_k w_k \langle \mathbf{E}_k(\mathbf{x}) \rangle,$$

$$\langle \mathbf{E}_m(\mathbf{x}) \rangle = \frac{1}{V_m} \int_{V_m} \mathbf{E}(\mathbf{x} + \boldsymbol{\xi})\, d\boldsymbol{\xi}, \qquad \langle \mathbf{E}_k(\mathbf{x}) \rangle = \frac{1}{v_k} \int_{v_k} \mathbf{E}(\mathbf{x} + \boldsymbol{\xi})\, d\boldsymbol{\xi},$$

where V_m is the matrix volume, v_k is the volume of the kth inclusion, f is the volume fraction of inclusions, w_k is f_k/f, and f_k is v_k/V. Similarly, the average polarization is given by

$$\langle \mathbf{P}(\mathbf{x}) \rangle = (1 - f)\langle \mathbf{P}_m(\mathbf{x}) \rangle + f \sum_k w_k \langle \mathbf{P}_k(\mathbf{x}) \rangle.$$

If we assume that constitutive relations of the form (2.23) are valid for the matrix and inclusions, it follows that

$$\langle \mathbf{P}_m(\mathbf{x}) \rangle = \varepsilon_0 \chi_m \langle \mathbf{E}_m(\mathbf{x}) \rangle, \qquad \langle \mathbf{P}_k(\mathbf{x}) \rangle = \varepsilon_0 \chi \langle \mathbf{E}_k(\mathbf{x}) \rangle,$$

where $\chi_m = \epsilon_m - 1$ is the susceptibility of the matrix and $\chi = \epsilon - 1$ is that of the inclusions. The average susceptibility tensor $\boldsymbol{\chi}_{\text{av}}$ of the composite medium is *defined* by

$$\langle \mathbf{P}(\mathbf{x}) \rangle = \epsilon_0 \boldsymbol{\chi}_{\text{av}} \cdot \langle \mathbf{E}(\mathbf{x}) \rangle,$$

where $\boldsymbol{\chi}_{\text{av}}$ is independent of position if the medium is statistically homogeneous. The preceding equations can be combined to yield

$$(1 - f)(\boldsymbol{\epsilon}_{\text{av}} - \epsilon_m \mathbf{1}) \cdot \langle \mathbf{E}_m(\mathbf{x}) \rangle + f \sum_k w_k (\boldsymbol{\epsilon}_{\text{av}} - \epsilon \mathbf{1}) \cdot \langle \mathbf{E}_k(\mathbf{x}) \rangle = 0, \quad (8.46)$$

where $\boldsymbol{\epsilon}_{\text{av}}$ is the average dielectric tensor and $\mathbf{1}$ is the unit tensor. Clearly, if $\boldsymbol{\epsilon}_{\text{av}}$ is to be independent of position, then $\langle \mathbf{E}_m \rangle$ and $\langle \mathbf{E}_k \rangle$ must be linearly related.

Consider an *isolated* ellipsoid in a *uniform* field $\mathbf{E}_m$; the uniform field $\mathbf{E}_k$ in the ellipsoid is given by $\mathbf{E}_k = \boldsymbol{\lambda}_k \cdot \mathbf{E}_m$, where the principal components of the tensor $\boldsymbol{\lambda}_k$ are (see Section 5.3)

$$\lambda_j = \frac{\epsilon_m}{\epsilon_m + L_j(\epsilon - \epsilon_m)} \qquad (j = 1, 2, 3).$$

With the *assumption*—and this is our major assumption—that the average fields are similarly related, that is, $\langle \mathbf{E}_k \rangle = \boldsymbol{\lambda}_k \cdot \langle \mathbf{E}_m \rangle$, (8.46) becomes

$$(1 - f)(\boldsymbol{\epsilon}_{\text{av}} - \epsilon_m \mathbf{1}) + f(\boldsymbol{\epsilon}_{\text{av}} - \epsilon \mathbf{1}) \cdot \sum_k w_k \boldsymbol{\lambda}_k = 0. \quad (8.47)$$

So our task reduces to that of determining the sum in (8.47); $\boldsymbol{\lambda}_k$ depends on the shape and orientation of the kth ellipsoid and w_k is the ratio of its volume to that of all ellipsoids. It is convenient to approximate the sum in (8.47) by an integral

$$\sum_k w_k \boldsymbol{\lambda}_k \simeq \int_k w(k) \boldsymbol{\lambda}(k)\, dk,$$

where the continuous variable k in the integral represents all the variables that specify an ellipsoid: shape, volume, and orientation. We now make several assumptions: there is no correlation between the volume of an inclusion and its shape or orientation; there is no correlation between shape and orientation; all orientations are equally probable. It follows from these assumptions that

$$\sum_k w_k \boldsymbol{\lambda}_k \simeq \beta \mathbf{1},$$

$$\beta = \int\int \mathcal{P}(L_1, L_2) \frac{\lambda_1 + \lambda_2 + \lambda_3}{3} dL_1\, dL_2, \tag{8.48}$$

where $\mathcal{P}(L_1, L_2)$ is the shape probability distribution function (see Section 12.2); the average (scalar) dielectric function is therefore

$$\epsilon_{av} = \frac{(1-f)\epsilon_m + f\beta\epsilon}{1 - f + f\beta}. \tag{8.49}$$

Note that (8.49), which is a generalization of the Maxwell Garnett dielectric function (8.50), is not invariant with respect to interchanging the roles of matrix and inclusions: if we make the substitutions $\epsilon \to \epsilon_m$, $\epsilon_m \to \epsilon$, and $f \to (1 - f)$, then ϵ_{av} is not, in general, unchanged. If, therefore, a two-component mixture is to be described by (8.49), a choice must be made as to which component is the matrix and which the inclusions (there may be physical reasons to guide this choice). The limiting values of ϵ_{av} are independent of β:

$$\lim_{f\to 1} \epsilon_{av} = \epsilon, \qquad \lim_{f\to 0} \epsilon_{av} = \epsilon_m.$$

It is not difficult to extend (8.49) or (8.47) to multicomponent mixtures. If we make the same assumptions for each inclusion that were made preceding (8.48), then the average dielectric function is

$$\epsilon_{av} = \frac{(1-f)\epsilon_m + \sum f_j \beta_j \epsilon_j}{1 - f + \sum f_j \beta_j},$$

where the volume fraction of the jth inclusion with dielectric function ϵ_j is f_j, $f = \Sigma f_j$, and β_j has the same form as (8.48) with ϵ replaced by ϵ_j.

It is instructive to expand (8.49) in powers of $\delta = \Delta/\epsilon_m$, where $\Delta = \epsilon - \epsilon_m$:

$$\epsilon_{av} = \epsilon_m \left[1 + f\delta - \frac{f(1-f)}{3}\delta^2 + \frac{f(1-f)\left(3\langle L^2\rangle - f\right)}{9}\delta^3 + \cdots \right],$$

$$\langle L^2 \rangle = \int\int \mathcal{P}(L_1, L_2)\left(L_1^2 + L_2^2 + L_3^2\right) dL_1\, dL_2.$$

To terms of order δ^2 the average dielectric function is independent of the shape of the inclusions. Also, to terms of order δ (8.49) is symmetric in matrix and inclusions. Bohren and Battan (1980) similarly expanded various average dielectric functions—Maxwell Garnett, Bruggeman (often called effective medium), Debye—and showed that they all agree to at least terms of order δ. Therefore, if we are dealing with mixtures the components of which are similar ($|\delta| \ll 1$), we need not worry unduly about which component to designate as the inclusions nor their shape. Neither need we agonize over which among the various competing expressions for the average dielectric function is best: any of them will do. A more stringent test of their relative merits would be how well they do for mixtures of very dissimilar substances.

If all the inclusions are spherical, $\beta = 3\epsilon_m/(\epsilon + 2\epsilon_m)$ and (8.49) reduces to

$$\epsilon_{av} = \epsilon_m \left[1 + \frac{3f\left(\frac{\epsilon - \epsilon_m}{\epsilon + 2\epsilon_m}\right)}{1 - f\left(\frac{\epsilon - \epsilon_m}{\epsilon + 2\epsilon_m}\right)} \right]. \tag{8.50}$$

The average dielectric function (8.50) was first derived by Maxwell Garnett (1904); subsequently, it has been rederived under various sets of assumptions (see, for example, Genzel and Martin, 1972, 1973; Barker, 1973; Bohren and Wickramasinghe, 1977).

The following expression for an average dielectric function was first obtained by Bruggeman (1935):

$$f\frac{\epsilon - \epsilon_{av}}{\epsilon + 2\epsilon_{av}} + (1 - f)\frac{\epsilon_m - \epsilon_{av}}{\epsilon_m + 2\epsilon_{av}} = 0. \tag{8.51}$$

Both the Maxwell Garnett and Bruggeman dielectric functions have been shown by Stroud (1975) to follow from the same integral equation: either one or the other is obtained depending on the approximations that are made. So we may consider (8.50) and (8.51) to be related: they issue from the same parent equation. Note that the Bruggeman dielectric function applies to a two-component mixture in which there are no distinguishable inclusions embedded in a definite matrix: both components are treated symmetrically. It might be more correct to say that it applies to a completely randomly inhomogeneous medium; it does not strictly apply to a particulate medium because there is no way to decide which component is the particles and which the surrounding medium. This difference between the Maxwell Garnett and Bruggeman theories shows up in comparisons with experimental data. Abeles and Gittleman (1976) measured transmission by the composite metal–insulator system Ag–SiO_2 and the composite semiconductor–insulator systems Si–SiC and Ge–Al_2O_3 and compared their results with calculations based on the two average dielectric functions. They concluded that only the Maxwell Garnett theory was compati-

ble with their observations. In particular, the $Ag-SiO_2$ transmission spectrum showed a band which the Bruggeman theory completely failed to predict. Although this band was not explicitly identified as a manifestation of surface mode excitation in silver particles, it is likely that this is so: we shall show in Section 12.4 that small silver particles can have strong shape-dependent absorption bands at visible and near-infrared wavelengths (see Fig. 12.18). As these bands depend very much on the particulate nature of the composite medium, it comes as no great surprise that the Bruggeman theory is inadequate in this instance. Landauer (1952), however, found good agreement between conductivities calculated from the Bruggeman theory and measured values, even for mixtures with components having greatly different conductivities. So it is certainly not true that the Maxwell Garnett theory is necessarily superior to the Bruggeman theory in every instance: both theories have their successes. Part of the ambiguity surely arises from the difference between a randomly inhomogeneous medium and one in which there are distinguishable inclusions embedded in a definite matrix.

Bohren and Battan (1980) tested the applicability of (8.50) and other average dielectric functions to inhomogeneous particles by calculating refractive indices of ice–water mixtures at a wavelength of 5.05 cm—the microwave dielectric functions of ice and liquid water are vastly different (Section 10.3). Radar backscattering calculations for ice spheres coated with ice–water mixtures were compared with measured cross sections. The evidence favoring the Maxwell Garnett theory over the Bruggeman theory was not compelling: both agreed reasonably well with measurements. Much more data needs to be gathered and analyzed, however, before the problem of scattering and absorption by inhomogeneous particles can be considered to have been "solved" (if, indeed, a general solution is possible). In the interim, we would be inclined to use (8.49) or (8.50) in small-particle calculations.

Measurements are sometimes made on inhomogeneous samples for which optical constants are inferred under the assumption of homogeneity and then used in all kinds of small-particle scattering and absorption calculations. For example, measured reflectances of inhomogeneous samples can be inverted to obtain optical constants from expressions which strictly apply only to homogeneous media (see Section 2.7). Now one cannot deny that this might give some sort of average optical constants. But they are certain to be applicable only to the exact experiment from which they were extracted. It would not generally be correct, for example, to use them in Mie calculations of scattering from a more or less spherical aggregation of inhomogeneous material.

Another kind of effective or average optical constants involves mixtures of different particles such as atmospheric aerosols or soils. Effective optical constants for compacted samples of these mixtures might be inferred from reflectance and transmittance measurements as if the samples were homogeneous. But scattering or extinction calculations based on these optical constants would not necessarily be correct.

An example of practical importance in atmospheric physics is the inference of effective optical constants for atmospheric aerosols composed of various kinds of particles and the subsequent use of these optical constants in other ways. One might infer effective n and k from measurements—made either in the laboratory or remotely by, for example, using bistatic lidar—of angular scattering; fitting the experimental data with Mie theory would give "effective" optical constants. But how *effectual* would they be? Would they have more than a limited applicability? Would they be more than merely consistent with an experiment of limited scope? It is by no means certain that they would lead to correct calculations of extinction; or backscattering; or absorption. We shall return to these questions in Section 14.2.

8.6 A SURVEY OF NONSPHERICAL PARTICLES, REGULAR AND IRREGULAR

Because homogeneous, spherical particles are the exception in nature rather than the rule, various exact and approximate methods have been devised for determining absorption and scattering by nonspherical particles, both those with regular shape (i.e., with boundaries specified by simple, smooth functions) and with irregular shape; some of these have already been discussed. Rayleigh theory and geometrical optics combined with diffraction theory, which are conceptually simple, apply to particles small and large compared with the wavelength, respectively. It is between these two limits where the major difficulties lie and to which most recent theoretical effort has been directed. Although it might be thought that all scattering problems are tractable by simple numerical methods, computational time can be excessive. Therefore, accurate and efficient methods for computing scattering by nonspherical particles are actively being developed.

The following is only a brief discussion of a few selected methods, their physical basis, advantages, and disadvantages. Further details may be found in the references cited. Yeh and Mei (1980) have given a succinct overview of some of these methods.

8.6.1 Separation of Variables

The classical method of solving scattering problems, separation of variables, has been applied previously in this book to a homogeneous sphere, a coated sphere (a simple example of an inhomogeneous particle), and an infinite right circular cylinder. It is applicable to particles with boundaries coinciding with coordinate surfaces of coordinate systems in which the wave equation is separable. By this method Asano and Yamamoto (1975) obtained an exact solution to the problem of scattering by an arbitrary spheroid (prolate or oblate) and numerical results have been obtained for spheroids of various shape, orientation, and refractive index (Asano, 1979; Asano and Sato, 1980).

Although this solution is exact it shares the drawbacks of other solutions for nonspherical particles: computations can be complicated and lengthy, particularly for larger particles and for averages over all orientations, not to mention size and shape distributions. Because of this, perhaps, the spheroid solution has been slow to be adopted by other workers. Nevertheless, the results of Asano and Sato (1980) give some of the best insights available into the systematic effects of nonsphericity in light scattering. Several examples from the work of Asano and his collaborators are included in Chapters 11 and 13.

8.6.2 Point Matching

In the point matching method (Oguchi, 1973; Bates, 1975) the fields inside and outside a particle are expanded in vector spherical harmonics and the resulting series truncated; the tangential field components are required to be continuous at a finite number of points on the particle boundary. Although easy to describe and to understand, the practical usefulness of this method is limited to nearly spherical particles; large demands on computer time and uncertain convergence are also drawbacks (Yeh and Mei, 1980).

8.6.3 Perturbation Methods

A nonspherical particle may be looked upon as a sphere the boundary of which is distorted, or "perturbed," by different amounts at different points. The field scattered by such a particle is, formally at least, given by an infinite series in a perturbation parameter the first term of which is the Mie solution. Perturbation solutions to the problem of scattering by nonspherical particles have been advanced by Yeh (1964) and by Erma (1968ab, 1969). The former author developed his theory only to first order in the perturbation parameter. The latter author claims an exact solution valid for all particles for which the series converge, without, however, specifying the conditions for convergence or giving numerical results so that the practicality of his method may be assessed. An infinite series solution that is formally exact is of little practical use unless it can be truncated after a reasonable number of terms without appreciable error. It seems likely that the practical usefulness of both these perturbation methods is limited to nearly spherical particles. This is a feature common to all perturbation methods: the further the system of interest deviates from the unperturbed system, the more terms are required and the more cumbersome and time consuming the computations become.

8.6.4 Purcell–Pennypacker Method

A solution to the problem of scattering by an arbitrary particle could be obtained in principle by computing the dipole moment induced in each of its constituent atoms by the incident field and the combined fields of all the other atoms. But even a small particle (say $\sim$ 1 μm) contains more than 10^{10} atoms,

which means that a comparable number of equations would have to be solved iteratively, clearly a formidable task. Purcell and Pennypacker (1973) adopted the basic methodology of this approach while reducing it to more manageable proportions.

A particle is subdivided into a small number of identical elements, perhaps 100 or more, each of which contains many atoms but is still sufficiently small to be represented as a dipole oscillator. These elements are arranged on a cubic lattice and their polarizability is such that when inserted into the Clausius–Mossotti relation the bulk dielectric function of the particle material is obtained. The vector amplitude of the field scattered by each dipole oscillator, driven by the incident field and that of all the other oscillators, is determined iteratively. The total scattered field, from which cross sections and scattering diagrams can be calculated, is the sum of all these dipolar fields.

Purcell and Pennypacker calculated scattering and absorption by various rectangular particles with different refractive indices for size parameters up to about two. More recently, Kattawar and Humphreys (1980) used the Purcell–Pennypacker method to investigate scattering by two spheres as a function of separation. Arbitrary shapes can be treated by this method but excessive computation time appears to preclude its use for large size parameters.

8.6.5 T-Matrix Method

A promising method based on an integral equation formulation of the problem of scattering by an arbitrary particle has come into prominence in recent years. It was developed by Waterman, first for a perfect conductor (1965), later for a particle with less restricted optical properties (1971). More recently it has been applied to various scattering problems under the name Extended Boundary Condition Method, although we shall follow Waterman's preference for the designation T-matrix method. Barber and Yeh (1975) have given an alternative derivation of this method.

In Chapter 4 a plane wave incident on a sphere was expanded in an infinite series of vector spherical harmonics as were the scattered and internal fields. Such expansions, however, are possible for arbitrary particles and incident fields. It is the scattered field that is of primary interest because from it various observable quantities can be obtained. Linearity of the Maxwell equations and the boundary conditions (3.7) implies that the coefficients of the scattered field are linearly related to those of the incident field. The linear transformation connecting these two sets of coefficients is called the T (for transition) matrix. If the particle is spherical, then the T matrix is diagonal.

Explicit expressions for the T matrix can be obtained by casting the scattering problem in integral rather than differential form. Details are given in the references cited above. We also recommend an expository article by Ström (1975).

Scattering by homogeneous spheroids and finite cylinders has been investigated by Barber and Yeh (1975) using the T-matrix method. Single coated prolate spheroids (Wang and Barber, 1979) as well as polydispersions of such particles (Wang et al., 1979) have also been treated. Because numerical results for particles of arbitrary shape and large volume can be obtained efficiently (Yeh and Mei, 1980) this method is actively being used at present.

8.6.6 The Need for a Statistical Approach

Many calculations for nonspherical particles have been, and are being, done with the methods outlined above. Although they may be quite suitable for single particles, ensembles of particles distributed in size, shape, and orientation are often of more interest. Of course, the properties of such ensembles follow from those of their individual members—but not trivially. With increasing dispersion, calculations can quickly escalate to unmanageable proportions, although heroic efforts have been made for randomly oriented, homogeneous (Asano and Sato, 1980) and inhomogeneous (Wang et al., 1979) spheroids.

We may imagine that an irregular particle is generated from a spheroid by chipping it at random. A spheroid requires four parameters for its characterization: two for size and shape, two for orientation. Each time a chip is made additional parameters are required. Even if an exact solution to the problem of scattering by such a chipped spheroid were obtainable, would it be of great value, particularly if we were interested only in the average properties of an ensemble of similar particles?

The effect of averaging over one or more particle parameters—size, shape, orientation—is to efface details: extinction fine structure, particularly ripple structure, to a lesser extent interference structure (Chapter 11); and undulations in scattering diagrams. If the details disappear upon averaging over an ensemble perhaps the best strategy in this instance would be to avoid the details of individual-particle scattering altogether and reformulate the problem statistically.

Further progress in the theory of light scattering by irregular particles may come from a statistical formulation of this problem. A small step in this direction is taken in Chapter 12, where extinction spectra of small irregular particles are approximated by averages over Rayleigh ellipsoids. The modest success of this approach suggests that it might profitably be extended to larger particles.

NOTES AND COMMENTS

The solution to the problem of scattering by a sphere described by the constitutive relations (8.5) was obtained by Bohren (1974). This was then extended to optically active spherical shells (Bohren, 1975) and cylinders (Bohren, 1978).

A good discussion of the dielectric properties of a mixture, independent of a specific model, has been given by Landau and Lifshitz (1960); we also recommend a paper by Niklasson et al. (1981) for its discussion of several aspects of the mixture problem.

An approach somewhat similar to that in Section 8.5 was taken by O'Neill and Ignatiev (1978), who obtained an expression for the average dielectric function of a mixture containing spheroidal inclusions with ratios of semiminor to semimajor axes given by a probability distribution function.

Further work on the theory of backscattering by inhomogeneous particles and its comparison with measurements has been done by Bohren and Battan (1981).

Banderman and Kemp (1973) have treated scattering by arbitrarily shaped particles in a manner similar to that of Purcell and Pennypacker (1973).

Some of the most recent work on scattering by irregularly shaped particles is contained in a collection of papers edited by Schuerman (1980).